DOWN*HOLE PHASE I: A COMPUTER MODEL FOR

PREDICTING THE WATER PHASE CORROSION

ZONE IN GAS AND CONDENSATE WELLS

By

CARL ALAN ROBERTSON

Bachelor of Science in Chemical Engineering
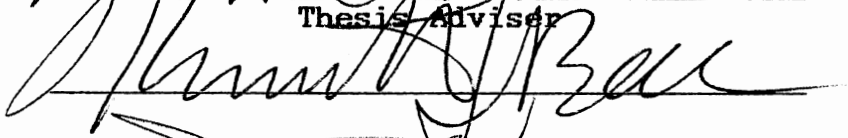
Oklahoma State University

Stillwater, Oklahoma

1986

Submitted to the Faculty of the
Graduate College of the
Oklahoma State University
in partial fulfillment of
the requirements for
the Degree of
MASTER OF SCIENCE
July 1988

DOWN*HOLE PHASE I: A COMPUTER MODEL FOR

PREDICTING THE WATER PHASE CORROSION

ZONE IN GAS AND CONDENSATE WELLS

Thesis Approved:

_____
Thesis Adviser

_____

_____

_____
Dean of the Graduate College

PREFACE

The DOWN*HOLE Production String Simulation Package is a user-friendly tool developed with the Corrosion Engineer in mind. The program is designed to determine the location of the water condensation zone in gas wells, and to predict the prevailing flow regime throughout the wet region. This system is a multicomponent two-phase flow pressure loss prediction tool. Two-phase pressure loss is determined by the Homogeneous [10], Orkiszewski [42], and Yao-Sylvester [61] flow methods.

ACKNOWLEDGMENTS

I would like to thank all of the people who helped me through my college career at Oklahoma State University. I am deeply indebted to Dr. Ruth Erbar for her constant encouragment, technical assistance, and wise counsel. This project would not have been possible without her help. I would also like to thank Dr. Kenneth J. Bell and Dr. Jan Wagner for their guidance.

Credit should also be given to Christopher Wero and Julia Finch for helping me maintain my sanity throughout the Graduate School experience.

This project was funded by The Materials Technology Group of ARCO Oil and Gas Company at Plano, Texas. I gratefully acknowledge the support of Dr. Ed Burger, Harry Byars, and Mark Mateer during the past months.

Finally, my father and brother deserve my admiration for their constant support, encouragement, and understanding.

TABLE OF CONTENTS

LIST OF TABLES

LIST OF FIGURES

NOMENCLATURE

A	flow area
A_c	gas core cross sectional area
A_p	flow area of pipe
D	tubing diameter
d_h	pipe hydraulic diameter
D_s	standard deviation about the mean percent error
E	dissipation of mechanical energy into heat, equation 10
E	percent error
E	mean percent error
F	number of degrees of freedom in a system
F	net force exerted by a homogeneous fluid in overcoming friction
F_e	Henstock-Hanratty dimensionless group
F_f	force exerted by liquid phase in overcoming friction
F_g	flowing gas fraction, equation
F_g	force exerted by vapor phase in overcoming friction
f_t	two-phase friction factor
f_{tp}	two-phase friction factor
G	mass flux
g	acceleration due to gravity
g_c	gravitational constant

i	fluid enthalpy
K	constant defined by equation 4
L_b	bubble-slug regime boundary
L_m	transition-mist boundary
L_s	slug-transition boundary
M_g	gas mass flow rate
M_{en}	entrained liquid mass flow rate
M_{lf}	annular liquid film mass flow rate
M_{lg}	mixture mass flow rate in core
M_{tl}	total liquid mass flow rate
M	gas molecular weight
n	number of wells
N_b	bubble Reynolds number
N_r	number of variables fixed by restraints on a system
N_{Re}	Reynolds number
$N_{Re,m}$	mixture Reynolds number
$N_{Re,g}$	gas Reynolds number
$N_{Re,1}$	liquid Reynolds number
N_s	number of variables which must be fixed to specify a system
N_t	number of recurring variables in a process
N_v	total number of degrees of freedom in a system
N_w	constant defined by equation 53
P	number of phases present in a degrees-of-freedom analysis
P	perimeter
p	pressure

p_c	calculated pressure drop
p_m	measured pressure drop
q_g	in-situ gas volumetric flow rate
q_l	in-situ liquid volumetric flow rate
T	temperature
u	average velocity of homogeneous fluid
u_f	actual velocity of liquid phase
u_g	actual velocity of vapor phase
v	average specific volume of homogeneous fluid
v_f	specific volume of liquid
v_g	specific volume of vapor
v_{fg}	difference in specific volumes of saturated liquid and vapor
V_m	in-situ mixture velocity
V_{sg}	in-situ superficial gas velocity
V_{sg}^*	superficial gas velocity required for annular-mist flow
V_e	erosional velocity
W	total mass flow rate
X	constant defined by equation 5
x	quality
Y	constant defined by equation 6
C	empirical constant in API RP 14E formula
z	length
β	dimensionless quantity in entrainment correlation
Γ	liquid distribution coefficient
δ	average effective film thickness
ϵ	absolute roughness

θ	angle of deviation from vertical
λ	in-situ core liquid holdup
μ_g	gas viscosity
μ_l	liquid viscosity
μ_m	mixture viscosity
v	fluid velocity
v_b	bubble rise velocity
v_{gd}	dimensionless gas velocity
v_s	slip velocity
$\bar{\rho}$	average density
ρ_g	gas density
ρ_l	liquid density
ρ_m	mixture density
σ	gas-liquid surface tension
τ_f	friction loss gradient
τ_w	wall shear stress

CHAPTER I

INTRODUCTION

Background

Corrosion in oil and gas wells is a serious problem. Operators incur great expenses due to production string failures, lost production due to downtime, high workover costs, and high costs of chemical inhibition [56].

Although sour gas has been produced for many years, the amount of sour gas produced has increased significantly since the Arab Oil Embargo of 1974 and the Iranian Crisis of 1979 [43]. Questions about the energy independence of the United States and its effect on the national security of this country were prevalent throughout the 1970's. Many political and psychological factors fostered an atmosphere whereby previously uneconomical hydrocarbon reserves could now be economically exploited. Most of this "new" energy was in the form of heavy sour crude oil or very sour natural gas in deep formations.

In the late 1970's and early 1980's deep hot gas wells were developed in the Tuscaloosa Trend of South Louisiana [26,33], the Whitney Canyon Field in the Over-

1

thrust Belt of Southwest Wyoming [34], the Foothills
Region of Alberta, Canada [47], and elsewhere. The number
of ultra-deep wells exceeded 100 for the first time in
1982. An ultra-deep well is a well which is 20,000 ft. or
deeper. The average cost of drilling an ultra-deep well
was about $11.42 million per well [39]. Virtually all of
the 132 ultra-deep wells drilled in 1982 were intended to
be gas wells. Another factor influencing the development
of hot sour gas reserves is the demand for elemental
sulfur. Current global demand for sulfur far exceeds that
available from producing wells. Thus, future development
of deep sour gas reserves as a source of sulfur is likely
[54].

The economic climate of the 1970's proved to be both
a blessing and a curse for many energy companies [43].
With the blessing of higher price for the product which
oil companies produced came the curse of higher operating
costs. The cost of corrosion to the petroleum industry
has been estimated at more than $800 million annually in
1983, with oil companies spending an additional $50
million per year on chemical inhibitors to control
corrosion at that time [8]. Much of this increased
operating cost took the form of corrosion inhibition and
control due to the increased production of sour oil and
gas.

Purpose

The purpose of this work is to develop an easy-to-use computer program which will predict the location of the water condensation zone in gas wells. The onset of water condensation is generally considered as the point in the string above which corrosion is most likely to occur [21,22].

This task was accomplished by combining an existing thermodynamic phase equilibrium calculation package with fluid flow calculation subroutines. The program, dubbed DOWN*HOLE, is most effectively used on wells which produce only condensed water.

Program History

The development of the DOWN*HOLE Production String Simulation Package began at Oklahoma State University in early 1986. Several industry representatives expressed interest in a computer model which could predict the location of the water phase condensation zone in the production string of gas and condensate wells. Subsequently, a literature survey was conducted and a study of the feasibility of developing such a system was initiated. The results of this study are documented in a report issued in May, 1986 [49]. The positive recommendations of this report resulted in the development of a research proposal for industry [19]. Due to the catastrophic collapse of the petroleum industry,

3

project funding was obtained from only a single sponsor, ARCO Oil and Gas Company Materials Technology Group.

The primary stumbling-block to the development of the simulator was the development of a thermodynamics package suitable for calculating phase behavior of produced fluids at potentially severe downhole conditions. Fortunately, a very reliable thermodynamic simulator is available through the Gas Processors Association. This package, known as GPA*SIM, was developed by Dr. John Erbar at Oklahoma State University [16]. GPA*SIM is especially convenient for this project because it already contains algorithms for performing dewpoint and flash calculations needed for DOWN*HOLE.

Development of DOWN*HOLE proceeded by making several alterations to GPA*SIM. A Master Menu was added, which provides a list of options to the user. Subroutines to automatically generate hydrocarbon-rich and water-rich dewpoint curves were also added. Algorithms were provided to perform flash calculations at separator, wellhead, and bottomhole conditions. These subroutines are included for the purpose of checking for water formation at each point in the system.

Major additions to GPA*SIM include pressure drop prediction subroutines. Two-phase flow conditions may exist in wells of interest. Three correlations are provided for calculating two-phase pressure drop in the production tubing. Also, a subroutine is included to

4

provide the user with a fluid velocity profile of the production string.

Finally, data from several wet gas wells were obtained from the literature. Program logic was checked by inspecting the source code and comparing hand calculations with program output.

CHAPTER II

CORROSION OVERVIEW

Introduction

Corrosion may be defined as the deterioration of a substance or its properties because of a reaction with the environment [63]. Corrosion may be separated into two major classes. The first class of corrosion is general corrosion. General corrosion consists of overall metal loss and general thinning of metal due to chemical or mechanical means.

Localized corrosion is the second major class of corrosion. This type of corrosion takes the form of pits, gouges, and grooves, and includes phenomena such as galvanic corrosion, concentration cell corrosion, fatigue, intergranular corrosion, stress-corrosion cracking, leaching, and many others.

The principal cause of corrosion in gas wells is the presence of liquid water [57]. Corrosion problems due to the presence of water in gas wells and gathering systems are well documented. Corrosion is initiated by low pH water contacting the surface of tubular goods in the absence of a protective oil wetting film. Some mechanical

6

degradation of tubulars may be attributed to a corrosion/ erosion phenomenon resulting from high fluid velocities [3,12,30,33,50]. Extremely high pressure and temperature may also have and effect on the corrosivity of produced fluids. Conditions as treacherous as 15,000 psi bottomhole pressures and 550°F bottomhole temperatures have been encountered in some deep hot sour reservoirs [28].

Corrosive Environments

Corrosive environments depend on the presence of an electrolyte. The most common electrolyte encountered in oil and gas production is water. Produced water may contain materials such as dissolved salts, acids, and gases, all of which may affect corrosion rates. The corrosion rate in any system is a function of the chemical and physical properties of the produced fluids and metals, as well as the temperature, pressure, gas/oil and water/oil ratios, and fluid velocity in the well.

Corrosion rates in oil and gas wells are influenced by many factors. These factors include temperature differentials, heat treatment of the metal, impurities in the metal, stress, potential differences, velocity, the presence of solids in produced fluids, differential concentration, sulfate reducing bacteria, and many others. Temperature differentials, improper heat treating, and impurities in the production string metal may provide an environment in which stresses are imposed on the production

7

string, many times resulting in catastrophic failure.

The result of excessive velocity, combined with the presence of solids (such as sand) in produced fluids may speed the rate of corrosion in production strings. Efforts have been made to quantify the effect of velocity on corrosion and to set an industry wide standard to limit these effects [3]. Biological factors such as the presence of sulfate reducing bacteria, and concentration gradients of acidic species may provide an environment conducive to the formation of concentration cells.

CHAPTER III

LITERATURE SURVEY

The DOWN*HOLE Production String Simulation Package is
composed of several major sections. Program requirements
include methods for calculating produced fluid thermo-
dynamic properties, transport properties, pressure drop,
and production string heat loss.

Several computer simulation packages exist which will
calculate flow characteristics and/or thermodynamic
properties for hydrocarbon systems. These models may be
grouped into two categories. The first is that group of
programs designed for general property prediction in pipe-
line, process design, and reservoir simulation applica-
tions. The second group of programs are those specifically
designed for application in the corrosion arena.

General Purpose Models

MAXFLOW

MAXFLOW is a fluid flow package designed to employ
nodal analysis techniques for maximizing productivity of a
well and reservoir system. This program was originally
developed at ARCO Oil and Gas Company Production Research

9

and has recently been modified by Garrett Computing
Systems, Inc. of Dallas, Texas [38].

The program was originally developed to use PVT
properties generated by the GPA*SIM thermodynamic
simulator. Modifications have since yielded a program
which can calculate PVT properties internally or read
property data in a data set. For system analysis, MAXFLOW
offers seven vertical two-phase flow correlations, four
horizontal two-phase flow correlations, four inflow
performance correlations as well as gaslift analysis,
completion analysis, choke, safety valve, deviated hole
options, and tubing or annular flow options.

Horizontal flow correlations available in MAXFLOW
include those developed by Beggs and Brill [7], Mukherjee
and Brill [41], and Eaton [14]. Vertical two-phase flow
correlations provided include those of Beggs and Brill [7],
Duns and Ros [13], Aziz [2], Gray [24], Orkiszewski [42],
Hagedorn and Brown [26], and Mukherjee and Brill [41].

Completion data may be entered to enhance the accuracy
of the model and provide information about reservoir
performance. Data entered with the completion option
includes drainage, wellbore, and damaged zone radii,
formation temperature and permeability, and perforation
geometric parameters. The Lasater [35] and the Vazquez and
Beggs [58] correlations are provided for calculation of the
dissolved gas/oil ratio, while methods of Standing [52] and
of Vazquez and Beggs [58] are provided for determination of

10

the oil formation volume factor.

This program was not developed for use in the field of corrosion and thus does not provide accurate methods for determining the water condensation zone in the production string.

TRAVERSE and OUTFLOW

TRAVERSE and OUTFLOW are pressure traverse programs developed for the IBM PC [32]. These programs determine flowing bottomhole or flowing surface pressures in wells experiencing two-phase flow conditions. TRAVERSE and OUTFLOW are mirror images of one another.

Two-phase flowing pressure estimates are made by dividing the production string into small increments so that average flow properties may be assumed. The correlation by Aziz et al. [2], is used to calculate pressure gradients in the slug flow regime. This correlation was chosen because it has similar accuracy to Orkiszewski's correlation, but is less complicated. The Duns and Ros gradient correlation is used for mist flow regime gradient predictions [13].

A special input option is provided to account for systems which are not completely vertical. Four special cases are allowed:

1. No deviation takes place at all
2. The well is vertical to a given depth and then deviates from vertical at a fixed angle to total measured depth,

11

3. The well is deviated initially at some fixed angle; at a given depth location, the well becomes vertical and remains vertical to total measured depth,

4. The well is vertical initially; at a specified depth location, the well deviates at a fixed angle until the top of a second and final vertical section is reached where the well then remains vertical to total depth.

The programs use vertical flow correlations exclusively and do not employ any inclined or horizontal flow correlations. Only the hydrostatic gradient term is adjusted to reflect true vertical displacements which occur in the deviated sections of the string.

PIPELINE

The PIPELINE program was developed at Oklahoma State University in 1981 as a tool for predicting flow behavior in pipelines [1]. The Soave-Redlich-Kwong equation of state (as programmed in GPA*SIM) is employed as the phase equilibrium calculation subroutine. Two-phase flow calculations may be performed for both horizontal and vertical flow. Correlations by Lockhart and Martinelli [37], the AGA-API [4], and Beggs and Brill [7] may be used for horizontal flow while the methods of Orkiszewski [42], Duns and Ros [13], and Beggs and Brill [7] are available for vertical flow configurations.

12

Viscosity calculations are performed based on the correlation of Thodos [46], while surface tension calculations are performed using equations presented in the GPSA Engineering Data Book [23]. This author was not able to obtain a copy of PIPELINE, but based on private conversations and information in the literature, this program was probably not tuned for use with two liquid phases present. This author also learned that this program was never completely debugged, and hence was probably never used in commercial applications.

Specific Programs

The University of Southwestern Louisiana
Model

This model is currently under development at the Corrosion Research Center at The University of Southwestern Louisiana at Lafayette. This program incorporates the Peng-Robinson equation of state in the phase equilibrium calculations. As of completion of the second phase of the program, six options are provided. They are [38]:

1) Temperature and pressure profiles of gas wells

2) Calculation of condensed water and formation water in a condensate well

3) Phase equilibrium model of a condensate well

4) Corrosion rate model

5) Film thickness model for annular two-phase flow, and

13

6)   Corrosion rate profile model.

Fluid Flow Correlations

Due to the wide range of fluid flow correlations used in the general applications programs, an extensive literature survey was conducted in the field.   This effort produced volumes of material, most of which is not applicable to this work.   Those works which were considered for use in this project are summarized below.

Poettmann and Carpenter [45]

This is a method for predicting the pressure traverse of flowing oil wells and gas lift wells assuming two phase flow behaves as a single average phase.   For flowing oil wells the procedure allows the calculation of the bottomhole pressure given only surface conditions.   For the case of gas lift wells, the depth, pressure, gas injection rate, and power requirements necessary to lift the oil may be determined.

Homogeneous Flow Method [10]

This procedure considers the two phases as a single phase with average properties.   This model is also known as the 'friction factor' or 'fog flow' model.   The three basic assumptions used in this model are

1)   equal vapor and liquid velocities,

2)   the attainment of thermodynamic equilibrium

14

between phases, and

3) the use of a single phase friction factor for two-phase flow.

This model should perform the best in flow situations which are characterized by an extremely large mass fraction of either liquid or vapor; that is, very high or very low quality flow.

Cornish [11]

This method was developed in an effort to accurately predict the pressure traverse of oil wells producing in excess of 5000 barrels per day. This procedure uses the general energy equation and assumes the two phases flow as a single phase with average properties. The standard Moody diagram is used to determine the friction factor, and the pressure traverse is evaluated using PVT data for the crude of interest. This correlation accounts for liquid holdup by modifying the average density accordingly.

Hagedorn and Brown [26]

This procedure is essentially the same as that of Cornish, but was developed for more conventional flow rates through small diameter conduits. This investigation appears to be more in-depth than that of Cornish. Several field tests were made using a 1500 ft. deep test well. The two-phase friction factor and holdup factor were correlated with pipe diameter and several dimensionless groups.

15

Baxendell and Thomas [6]

This correlation was developed for predicting pressure gradients in high flow rate wells which were produced through the casing-tubing annulus. This simple method assumes the two phases flow as one, and does not account for liquid holdup.

Tek [55]

This investigator developed a graphical method for predicting the pressure traverse in flowing oil wells and gas lift wells. This method is essentially identical to that of Poettmann and Carpenter, but with the novel twist of the graphical solution.

Orkiszewski [42]

This procedure is a regime-dependent pressure loss prediction method. The entire realm of flow is separated into four regimes; bubble, slug, slug to annular-mist transition, and annular mist. The bubble-slug regime boundary is defined by Griffith and Wallis [25], while the Duns and Ros map is used for the three remaining regimes [13].

Chierici, Ciucci, and Sclocchi [9]

This method is similar to that of Orkiszewski in that the pressure loss depends on the prevailing flow regime. The major difference between this method and Orkiszewski's

16

procedure lies in the definition of constants in the slug flow regime. Evidence shows the definitions used by Orkiszewski are superior [9].

Yao and Sylvester [61]

This model assumes flow to be in the annular-mist regime as defined by Taitel, Barnea, and Dukler [53]. The fraction of liquid entrained in the gas core is calculated by the Wallis method [59]. The in-situ liquid holdup is determined knowing the entrainment factor and the volumetric flow rate of each phase. Average physical properties are determined from the liquid holdup, and the pressure loss is then calculated.

CHAPTER IV

DISCUSSION

Introduction

This chapter discusses the basic philosophy used in the development of the DOWN*HOLE Production String Simulation Package. The theoretical bases of the models are explained in detail in the first part of the chapter. The second part of the chapter contains the program logic and limitations, and outlines a method for prudent use of the system.

Theoretical Aspects of the Model

Method

As described in a previous chapter, the purpose of this work is to develop a model to predict fluid phase behavior and flow characteristics at selected points in the production tubing of wet gas and condensate wells. We are specifically interested in predicting the water-wet zone in the well so as to determine the region where corrosion is most likely to occur. In addition, if the well produces both hydrocarbon liquid and water, we would like to predict local water/oil ratios.

The above task is accomplished by modelling the

18

production string as a series of consecutive flash drums (see Figure 1). This approach is similar to that used by Reinhardt at the University of Southwestern Louisiana [47]. Downhole conditions are predicted by integrating the appropriate set of mass, energy and momentum balance equations between wellhead and bottomhole conditions.

The Gibbs Phase Rule is given by:

$$P+F=C+2 \tag{1}$$

where

    P = number of phases present

    C = number of components present, and

    F = number of degrees of freedom in the system.

Erbar [15] outlines an easy to use method for determining the necessary number of fixed variables in a system by rewriting the Phase Rule as:

$$N_s = N_v - N_r + N_t \tag{2}$$

where

    N_s = the number of variables which must be fixed to uniquely specify the system,

    N_v = the total number of degrees of freedom in the process,

    N_r = the number of variables fixed by restraints on the system, and

    N_t = the number of recurring variables in the process.

19
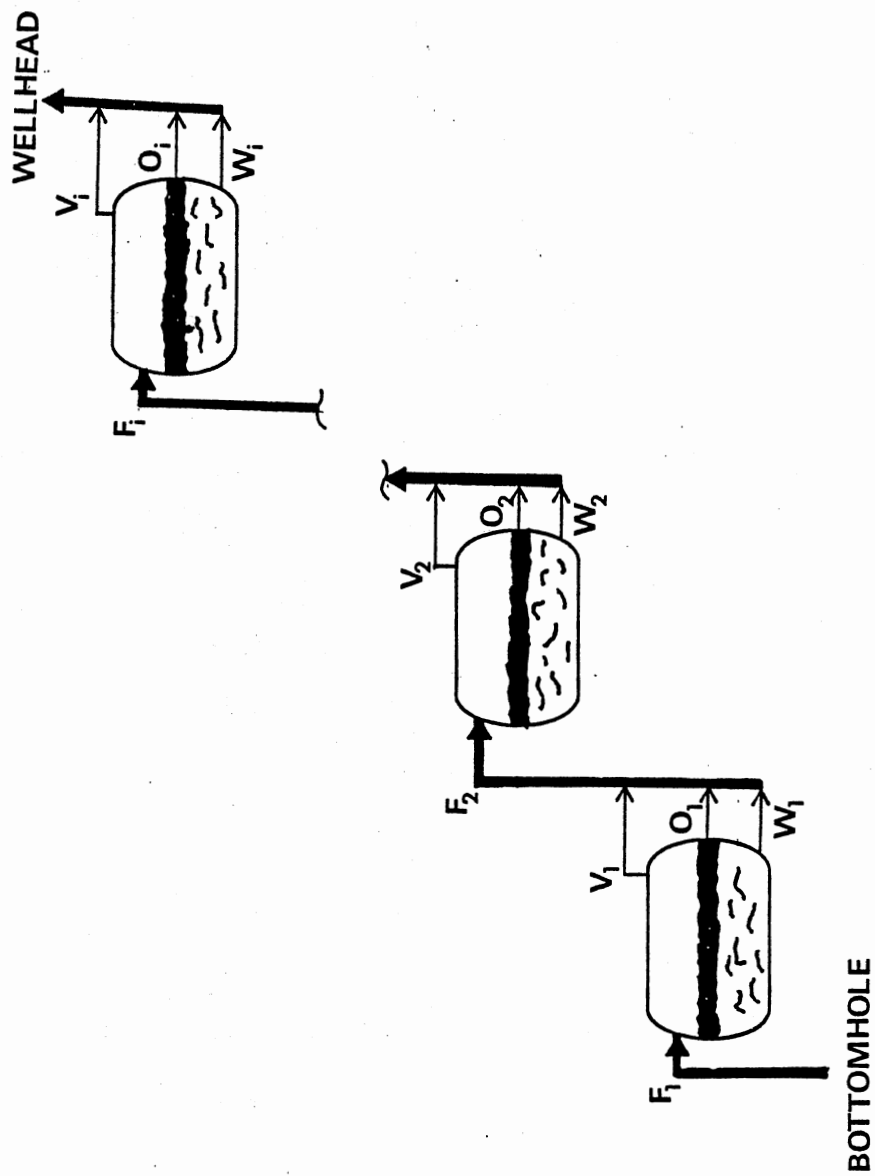
Figure 1. Production String Simulated As A Series Of Flash Drums.

For a single stream, the number of independent variables is C+2. Using this type of analysis, consider a single flash drum at any point in the production string model. This flash is assumed to contain a vapor phase and one liquid phase. The variable analysis is:

Independent Variable	N_v
Stream F	C+2
Stream L	C+2
Stream V	C+2
Heat Leak, q	1
Total	3C+7

Restraints imposed on the system are:

Restraints	N_r
Component Material Balance	C
Phase Distribution Relationship [C(P-1)]	C
Overall Energy Balance	1
Implied Temperature and Pressure of Streams L and V	2
Total	2C+3

Using the relationship of equation (2), it is obvious we must specify C+4 variables. The desired specification is:

Specified Variable	N_s
Stream F	C+2
Heat Leak, q	1

21

Flash drum Pressure or Temperature	1
Total	C+4

A similar analysis of a 3 phase flash producing a water-rich liquid phase is:

Independent Variable	N_v
Stream F	C+2
Stream L_1	C+2
Stream L_2	C+2
Stream V	C+2
Heat Leak, q	1
Total	4C+9

Restraints imposed on the system are:

Restraint	N_r
Component Material Balance	C
Phase Distribution Relationship [C(P-1)]	2C
Overall Energy Balance	1
Implied Temperature and Pressure Equalities	4
Total	3C+5

Subtracting the number of system restraints from the independent variables reveals that

$$N_s = C+4 \quad .$$

The desired specified variables are the same as with

the two-phase flash.

From the phase rule analysis we see that we must specify a combination of any two variables from a choice of pressure, temperature, or enthalpy. The complex flow calculations use flash calculations coupled with temperature or enthalpy specified iterative pressure calculation. Thus, the flash calculation determines the equilibrium temperature in the imaginary flash drum.

Property Prediction

Phase Equilibrium Calculations

Accurate thermodynamic equilibrium calculations are essential to properly predict local downhole compositions of all phases. In addition, the phase equilibrium calculation will determine the quantity of each phase present.

The GPA*SIM program is utilized as the phase equilibrium calculation subroutine in DOWN*HOLE [16]. GPA*SIM is capable of performing flash, dewpoint, and bubble point calculations. The program uses the Soave-Redlich-Kwong equation of state. Soave modified the popular Redlich-Kwong equation of state in the early 1970's [51]. The result was a cubic equation of state which could generally predict vapor pressures within 2%, compared to deviations ranging from a few percent to several hundred percent from the unmodified equation [60].

Erbar and co-workers [17,18] have since fitted their own coefficients and modified the SRK by developing binary

23

interaction parameters for a wide range of conditions. The
resulting modifications produced an equation which predicts
enthalpy departures to an average error of about 2 BTU/Lb
for defined hydrocarbon mixtures [18].

Density Calculations

High quality phase density calculations are necessary
in order to provide an accurate estimate of pressure drop in
the production string. The SRK equation of state in GPA*SIM
predicts vapor phase densities to within about 4-5%. Liquid
phase densities are predicted by the Hankinson-Thomson
COSTALD procedure [29]. The original test of the COSTALD
procedure yielded an astounding average absolute error of
0.37% over 4500 data points. Experience has shown that
prediction to about ±2-4% is a more realistic expectation
[18].

Viscosity Calculations

Accurate prediction of viscosities, as with densities,
is essential for determining pressure drop. Lee, Gonzales,
and Eakin developed a method to predict natural gas
viscosity based on gas density [36]. The correlation
reproduced experimental data for hydrocarbon systems to
within ±5% over a temperature range from 100 to 340°F and
pressures from 1000 to 8000 psia. The correlation is given
by the following set of equations:

$$\mu = K \exp\{X\rho^Y\} \qquad (3)$$

where

$$K = \frac{[\ 7.77 + 0.0063M\ ]\ T^{1.5}}{[\ 122.4 + 12.9M + T\ ]} \tag{4}$$

$$X = 2.57 + \frac{1914.5}{T} + 0.0095M \tag{5}$$

$$Y = 1.11 + 0.04X \tag{6}$$

T = absolute temperature of the system of interest, ^{O}R, and,

M = the molecular weight of the gas of interest.

The correlation covers the general temperature and pressure ranges of interest in this project.

Liquid viscosity is taken to be that of saturated liquid water at the temperature of interest. This approximation is justified by the fact that wells for which this program is designed produce little or no hydrocarbon liquids.

Surface Tension Prediction

Surface tension information is required by the regime-dependent two-phase flow pressure drop correlations. Surface tension is used in the calculation of the entrainment factor and vapor-liquid interface roughness. Surface tension is taken to be that of water at the desired temperature.

25

Pressure Drop Prediction

Introduction and Strategy

The simulator provides seven methods to model downhole conditions. These include the simple linear pressure profile, a two-phase homogeneous flow method, the Orkiszewski flow regime dependent correlation, and the Yao-Sylvester mist-annular flow regime method. Either the temperature or the enthalpy profile may be specified in the last three pressure drop prediction methods.

The Linear model assumes the pressure and temperature profiles to be linear between the wellhead and bottomhole. Flashes are performed at user-specified points in the production string to check for water.

The remaining three models assume a either a linear fluid enthalpy profile or a linear temperature profile down the well, calculate pressure with the desired method, then perform the flash calculation.

The models are intended to be used in conjunction with one another. The linear model should be used as a "first pass" calculation, followed by the Homogeneous, Orkiszewski, and Yao-Sylvester methods.

Flow Regimes

Collier [10] presents a description of flow patterns encountered in vertical upward co-current flow. Each pattern is shown in Figure 2 and is described in detail

26

Bubbly   Slug   Churn   Wispy--   Annular
                           Annular
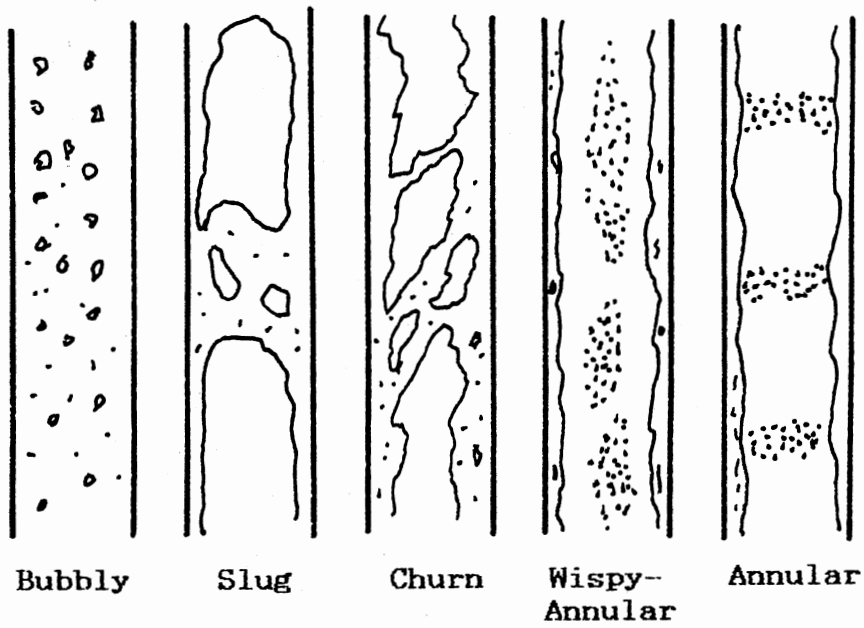
Figure 2.   Flow Patterns As Defined By Collier
            (After Collier [10]).

below. This information is presented in an attempt to familiarize the reader with such flow patterns and to prevent confusion in the next sections of the text.

Bubbly Flow [10]. In this regime the gas phase is distributed as discrete bubbles in a continuous liquid phase. Bubble description ranges from small and spherical to large cap-shaped. The latter state may be confused with slug flow as the bubble diameter approaches that of the pipe.

Slug Flow [10]. In slug flow gas bubbles are approximately the diameter of the pipe. The nose of the bubble is spherical and the gas in the bubble is separated from the pipe wall by a slowly descending film of liquid. The large gas bubbles are generally separated by slugs of liquid which may or may not contain small spherical bubbles.

Churn Flow [10]. Churn flow is formed by the breakdown of the large gas bubbles in slug flow. The gas flows in a more or less chaotic manner through the liquid which is generally displaced to the pipe wall. The flow oscillates with time. This regime may be referred to as semi-annular or slug-annular flow.

Wispy-annular Flow [10]. Wispy-annular flow takes the form of a relatively thick liquid film on the pipe walls together with a considerable amount of liquid entrained in a central gas core. Small gas bubbles may be present in

the liquid film, and entrained liquid appears as large droplets which have combined to form long irregular filaments or wisps.

Annular Flow [10]. Annular flow is characterized by a liquid film on the walls of the pipe with a continuous central gas core. Large amplitude waves may be present on the surface of the liquid film, forming a source for droplet entrainment in the gas core.

Homogeneous Flow Method [10]

This method is used to calculate pressure losses in two-phase flow by assuming the two phases behave as a single phase with average fluid properties. Major assumptions implied in the model are:

1)   equal vapor and liquid velocities,

2)   Liquid and vapor phases have achieved
       thermodynamic equilibrium, and

3)   a single phase friction factor for two-phase flow
       is suitably defined.

These assumptions appear to be valid for the cases of large liquid and small vapor flow rates, and vice versa. That is, this pressure drop prediction method is most accurate for wells which flow in the bubble or annular flow regimes.

Starting with the assumption of steady state flow, the Homogeneous Flow Method may be developed from the equations of continuity, momentum, and energy. These equations in

29

reduced form are, respectively

$$W = A\bar{\rho}\bar{u} \tag{7}$$

$$-Adp - d\bar{F} - A\bar{\rho}g \sin\theta \, dz = Wd\bar{u} \tag{8}$$

$$\delta q - \delta w = di + d\left(\frac{\bar{u}^2}{2}\right) + g \sin\theta \, dz \tag{9}$$

where

$$di = \delta q + dE + \bar{v}dp \tag{10}$$

The average specific volume is defined as

$$\bar{v} = v_f + xv_{fg} = \frac{1}{\bar{\rho}} \tag{11}$$

Assumption (1) above tells us the following:

$$\bar{u} = u_f = u_g \tag{12}$$

The total wall shear force, $d\bar{F}$, can be expressed as a wall shear stress, τ_w, acting over the inside of the channel:

$$d\bar{F} = \tau_w Pdz \tag{13}$$

where

$$\tau_w = f_{tp} \left(\bar{\rho} \, \bar{u}^2 / 2 \right) \tag{14}$$

and

P = wetted perimeter.

The net frictional force acting on each phase can be expressed in terms of the areas occupied by each phase:

$$dF_g + S = -A_g \frac{dp}{dz} gF \ dz \qquad (15)$$

$$dF_f - S = -A_f \frac{dp}{dz} fF \ dz \qquad (16)$$

Thus,

$$dF_f + dF_g = -A \frac{dp}{dz} F \ dz \qquad (17)$$

Rearranging equation (17) and substituting

$$dF = dF_g + dF_f \qquad (18)$$

results in the following equation:

$$- \frac{dp}{dz} F = \frac{1}{A} \frac{dF}{dz} \qquad (19)$$

Substituting equation (13) into (19) produces the following expression:

$$- \frac{dp}{dz} F = \frac{\tau_w P}{2} \qquad (20)$$

If τ_w is replaced by equation (10) and a circular channel geometry is assumed, the pressure loss due to friction is expressed as

$$- \frac{dp}{dz} F = \frac{2f_{tp} G^2 \bar{v}}{D} \qquad . \qquad (21)$$

31

The contribution to the total pressure loss by the acceleration gradient is given by the following expression:

$$- \frac{dp}{dz} a = G^2 \frac{d(\bar{v})}{dz} \tag{22}$$

The static head contribution is given by

$$- \frac{dp}{dz} z = \bar{\rho} g \sin\theta = \frac{g \sin\theta}{\bar{v}} \tag{23}$$

Combining equations (21), (22), and (23) to form a total pressure loss term yields

$$\frac{dp}{dz} = \frac{\frac{2f_{tp} G^2 v_f}{D} \left[1 + x \frac{v_{fg}}{v_f} \right] + G^2 v_f \frac{v_{fg}}{v_f} \frac{dx}{dz} + \frac{g \sin\theta}{v_f \left[1 + x \frac{v_{fg}}{v_f} \right]}}{1 + G^2 x \frac{dv_g}{dp}} \tag{24}$$

The friction factor is assumed to be a function of the Reynolds number:

$$f_{tp} = 0.079 \left[\frac{GD}{\mu} \right]^{-1/4} \tag{25}$$

Two additional simplifying assumptions have been made. First, the gas phase compressibility is neglected. Secondly, the production string is divided into a large enough number of increments so that the acceleration gradient over each increment may be neglected. Thus, the simplified pressure drop equation is

$$- \frac{dp}{dz} = \frac{2f_{tp}G^2\bar{v}}{D} + \frac{g\sin\theta}{\bar{v}} \tag{26}$$

The model is used to evaluate pressure losses in the production string by numerically integrating equation (26) over the length of the string.

The Orkiszewski Method

The Orkiszewski correlation [42] is a complex regime-dependent pressure loss prediction method. This correlation is a combination of work done by Duns and Ros [13] and by Griffith and Wallis [25]. The method is capable of predicting two-phase pressure losses with an accuracy of about 10 percent.

The regime- and holdup-dependent method considers only the four flow regimes of bubble, slug, annular-slug transition, and annular mist (See Figure 3). Obviously, this type of classification is not as intricate as that of Collier. Colliers' churn regime is analogous to the annular slug regime of Orkiszewski. In addition, Colliers' wispy-annular and annular flow regimes are apparently lumped together in Orkiszewski's annular-mist regime.

The flow regime map of Duns and Ros (shown in Figure 4) is used in this correlation. The boundary between bubble and slug flow is defined by Griffith and Wallis. Flow regime boundaries are given by the following equations:

Limits	Flow Regime
$q_g/q_t < L_b$	Bubble

33

| BUBBLE | SLUG | TRANSITION | ANNULAR - MIST |
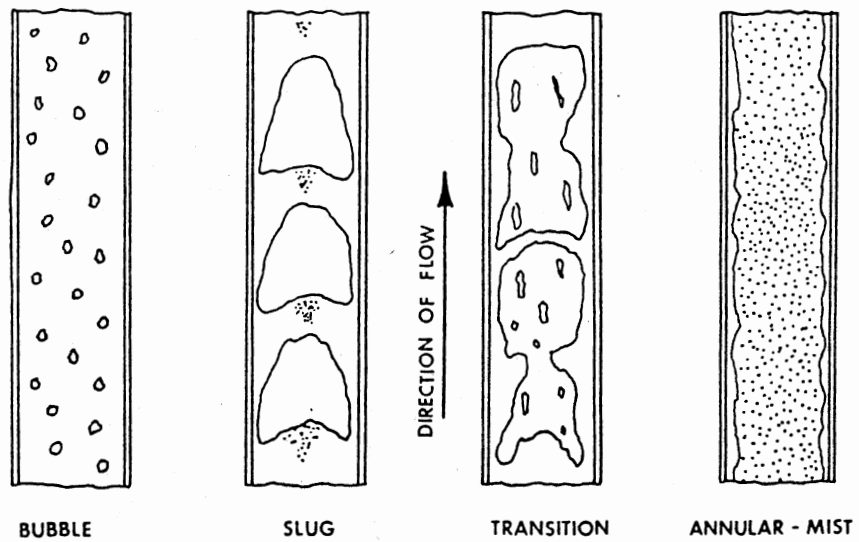
Figure 3.   Flow Patterns Used By Orkiszewski
(After Orkiszewski [42]).
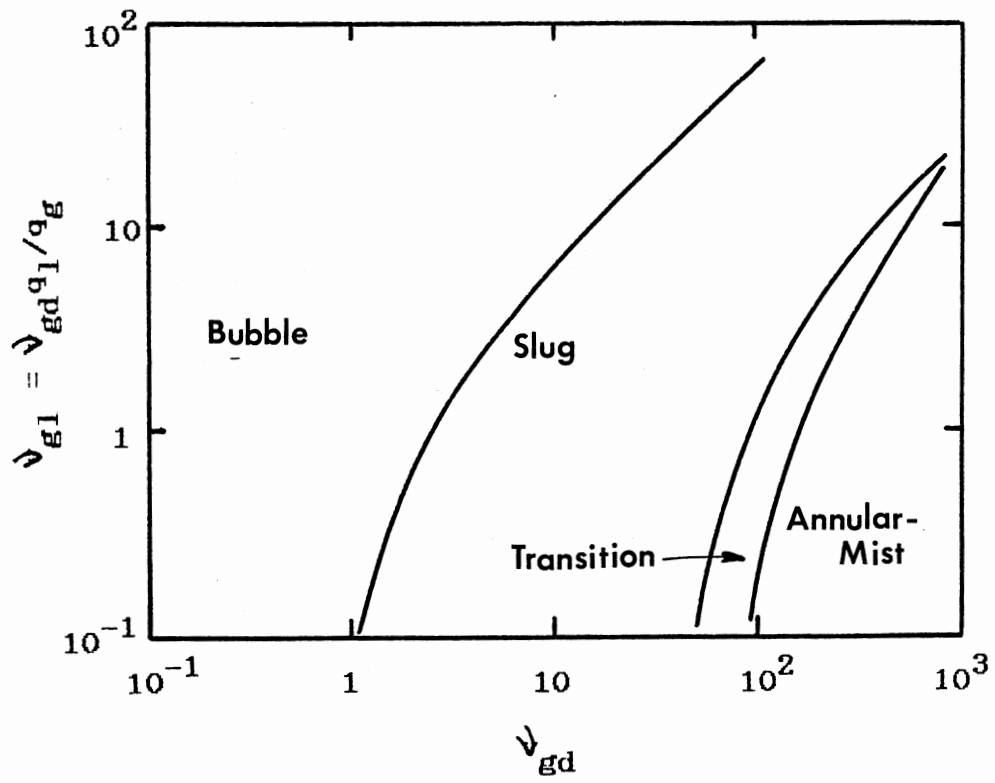
Figure 4.   Flow Regime Map Of Duns and Ros
(After Duns and Ros [13]).

35

$$q_g/q_t > L_b \text{ and } v_{gd} < L_s \qquad \text{Slug}$$

$$L_m > v_{gd} > L_s \qquad \text{Transition}$$

$$v_{gd} > L_m \qquad \text{Mist}$$

where L_b, L_s, and L_m are boundaries for bubble, slug, and mist regimes defined by:

$$L_b = 1.071 - \frac{(0.2218 \, v_t^2)}{d_h} \tag{27}$$

with the limit

$$L_b >= 0.13$$

$$L_s = 50 + 36 \, v_{gd} \frac{q_l}{q_g} \tag{28}$$

$$L_m = 75 + 84 \, v_{gd} \frac{q_l}{q_g}^{0.75} \tag{29}$$

and

$$v_{gd} = \frac{q_g}{A_p} \left(\frac{\rho_l}{g\sigma} \right)^{0.25} \tag{30}$$

This correlation is based on the premise that the general energy balance equation holds for all regimes. This equation, given as:

$$-dp = \tau_f \, dz + \frac{g\rho}{g_c} dz + \frac{\rho v}{g_c} dv \tag{31}$$

is composed of terms which account for frictional losses and

changes in potential and kinetic energy. The last term in the energy balance equation, that of kinetic energy change, is significant only in vapor shear controlled flow regimes. Thus, the acceleration term may be re-expressed as

$$\frac{\rho \nu}{g_c} \, d\nu = -\frac{w_t q_g}{g_c A_p^2 p} \, dp \tag{32}$$

The general equation is evaluated by incrementing the flow string such that the physical properties of the fluid do not change appreciably over the increment. The flow regime of the increment is determined and appropriate values for $\bar{p}$ and $\hat{v}_f$ are calculated based on the regime present in the increment. Obviously, this procedure is iterative in nature. Methods of evaluating friction loss gradient and average density in each regime are presented below.

Bubble Flow. Pressure drop calculation in the bubble flow regime requires knowledge of the amount of gas phase flowing along with the liquid. The void fraction is expressed by the following equation:

$$F_g = \frac{1}{2} \left[1 + \frac{q_t}{v_s A_p} - \sqrt{\left(1 + \frac{q_t}{v_s A_p} \right)^2 - \frac{4 q_g}{v_s A_p}} \right] \tag{33}$$

The slip velocity, $\hat{v}_s$, is taken as 0.8 ft/sec.

The average flowing density is calculated from the following equation:

37

$$\bar{\rho} = (1 - F_g)\rho_1 + F_g\rho_v \tag{34}$$

The friction loss gradient is determined from:

$$\tau_f = \frac{f\,\rho_1 \nu_1^2}{2g_c d_h} \tag{35}$$

This is based on liquid flowing properties since liquid comprises most of the total flowing mass in bubble flow. However, the friction loss gradient is corrected for the presence of bubbles in the velocity term. The flowing velocity is calculated based on an equivalent flowing area of the liquid:

$$\nu_1 = \frac{q_1}{A_p(1-F_g)} \tag{36}$$

Slug Flow. The concept of predicting pressure losses in this regime is simple, but the intricate details of the calculation are much more complex than for other regimes. The average density and friction loss gradient are functions of the bubble rise velocity, $\vec{\nu}_b$, and the liquid distribution coefficient, Γ.

The bubble rise velocity for slug flow is a function of the bubble Reynolds number, N_b, and is given by the following expression:

$$\nu_b = (0.546 + 8.74 \times 10^{-6} N_{Re})(g d_h)^{1/2} \tag{37}$$

for

$N_b < 3000$,

$$\nu_b = (0.35 + 8.74 \times 10^{-6} N_{Re})(gd_h)^{1/2} \tag{38}$$

for

$N_b > 8000$,

and

$$\nu_b = \frac{1}{2}\left(\nu_{b1} + \sqrt{\nu_{b1}^2 + \frac{13.59\,\mu_1}{\rho_1\,(d_h)^{1/2}}}\,\right) \tag{39}$$

for

$3000 < N_b < 8000$

where

$$\nu_{b1} = (0.251 + 8.74 \times 10^{-6} N_{Re})(gd_h)^{1/2} \tag{40}$$

and

$$N_b = 1488\,\nu_b d_h \rho_1 / \mu_1 \tag{41}$$

This set of equations is solved by assuming a value for the bubble rise velocity, calculating the bubble Reynolds number, and repeating the procedure until the bubble velocity converges within a desired tolerance.

The liquid distribution coefficient is an empirical parameter designed to account for several physical effects. First, liquid may be distributed in three places: in the slug, in the film around the gas bubble, and entrained mist in the gas bubble. Secondly, the contribution to friction

39

loss comes from the liquid film surrounding the gas bubble and the liquid slug. Finally, the limiting case of mist flow implies that the bubble rise velocity approaches zero.

Liquid distribution coefficients for water as determined by Orkiszewski, are given by the following equations:

$$\Gamma = [(0.013\log\mu_l)/d_h^{1.38}] - 0.681 + 0.232\log v_t - 0.428\log d_h \tag{42}$$

for

$$v_t < 10$$

or

$$\Gamma = [(0.045\log\mu_l)/d_h^{0.799}] - 0.709 - 0.162\log v_t - 0.888\log d_h \tag{43}$$

for

$$v_t > 10$$

but limited by:

$$\Gamma \,|> -0.065 v_t \tag{44}$$

when

$$v_t < 10$$

and

$$\Gamma \,|> -\frac{v_b A_p}{q_t + v_b A_p}\left(1 - \frac{\bar{\rho}}{\rho_l}\right) \tag{45}$$

when

$v_t > 10$

The average fluid density for slug flow is given by

$$\bar{\rho} = \frac{w_t + \rho_1 \nu_b A_p}{q_t + \nu_b A_p} + \Gamma \rho_1 \tag{46}$$

The friction loss gradient is given by

$$\tau_f = \frac{f \rho_1 \nu_t^2}{2 g_c d_h} \left[\frac{q_1 + \nu_b A_p}{q_t + \nu_b A_p} + \Gamma \right] \tag{47}$$

This form is analogus to the single phase friction loss gradient with a correction factor added to account for the presence of two distinct phases.

Mist Flow. The average flowing density in this regime is a weighted average of liquid and vapor densities. Thus,

$$\bar{\rho} = (1 - F_g) \rho_1 + F_g \rho_g \tag{48}$$

where

$$F_g = \frac{1}{1 + \dfrac{q_1}{q_g}} \tag{49}$$

The simplified version of the void fraction equation is justified by the fact that almost no phase slippage occurs in mist flow.

The friction loss gradient for this regime is calculated from the following equation:

$$\tau_f = \frac{f \rho_g \nu_g^2}{2 g_c d_h} \tag{50}$$

41

The friction factor is obtained from the Colebrook equation [44], using wall roughness estimates given by

$$\frac{\epsilon}{D} = \frac{34\sigma}{\rho_g \nu_g^2 d_h} \tag{51}$$

for

$$N_w < 0.005$$

and

$$\frac{\epsilon}{D} = \frac{174.8 \, \sigma \, N_w^{0.302}}{\rho_g \nu_g^2 d_h} \tag{52}$$

for

$$N_w > 0.005$$

where

$$N_w = 4.52 \times 10^{-7} \left(\frac{\nu_g \mu_l}{\sigma}\right)^2 \frac{\rho_g}{\rho_l} \tag{53}$$

Transition Flow. The nature of the flow in the slug-mist transition zone is very chaotic. Thus, any rigorous analysis of this regime would likely yield a correlation of great complexity and questionable accuracy. Thus, the friction loss gradient and average density are linearly weighted with respect to the slug and annular-mist regimes. Hence, the equations are of the following form:

42

$$\bar{\rho} = \frac{(L_m - \nu_{gd})}{(L_m - L_s)} \bar{\rho}_{slug} + \frac{(\nu_{gd} - L_s)}{(L_m - L_s)} \bar{\rho}_{mist} \tag{54}$$

and

$$\bar{\tau}_f = \frac{(L_m - \nu_{gd})}{(L_m - L_s)} \tau_{f,slug} + \frac{(\nu_{gd} - L_s)}{(L_m - L_s)} \tau_{f,mist} \tag{55}$$

The Yao-Sylvester Annular-Mist Pressure Loss Model

The Yao-Sylvester correlation is a mechanistic model for predicting pressure loss in two-phase annular-mist vertical flow [61]. This model is based on the transition to annular mist flow developed by Taitel et al. [53]. The flow pattern map developed by Taitel is shown in Figure 5. This map is based on water-air upflow in a 5.1 cm diameter pipe. The annular-mist regime is said to exist if the following condition is met:

$$V_{sg}^* \, |> 3.1 \left[\frac{\sigma g (\rho_l - \rho_g)}{\rho_g^2} \right]^{1/4} \tag{56}$$

During annular-mist flow, some fraction of the liquid will be entrained in the gas core. This entrained fraction is given by:

$$F_e = 1 - \exp\{-0.125(\beta - 1.5)\} \tag{57}$$

where

$$\beta = \frac{3048 V_{sg} \mu_g}{\sigma} \left(\frac{\rho_g}{\rho_l} \right)^{1/2} \tag{58}$$
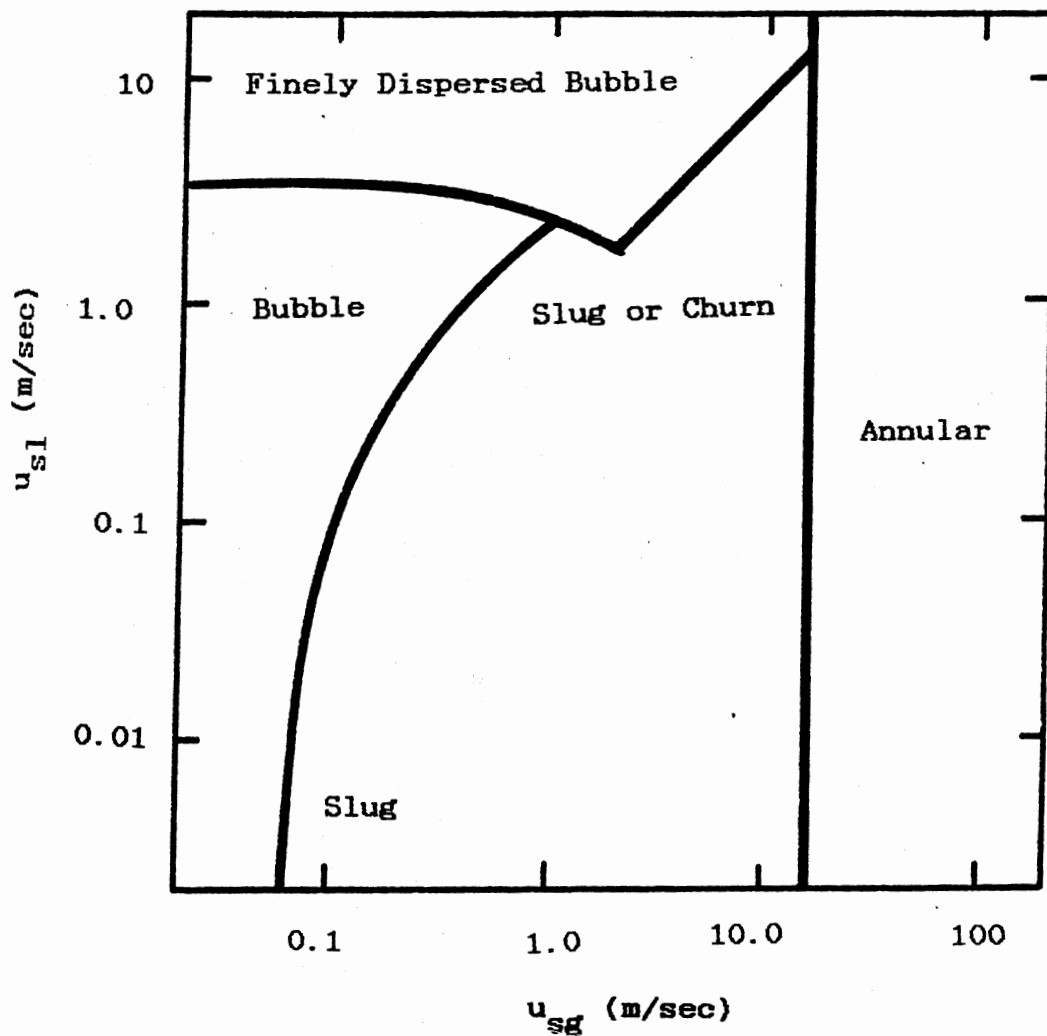
Flow Pattern Map for Vertical Tubes 5.0 cm. dia.,
air-water system at 25°C, 10N/sq.cm.

Figure 5.   Flow Regime Map Proposed by
            Taitel, Barnea, and Dukler
            (After Taitel et al. [53]).

Once the fraction of liquid entrained in the gas core is determined, the density of the gas core is calculated from

$$\rho_m = \lambda \rho_1 + (1-\lambda)\rho_g \qquad (59)$$

where

$$\lambda = \frac{F_e q_1}{F_e q_1 + q_g} \qquad (60)$$

The actual flowing gas velocity may be greater than the superficial velocity if annular flow exists. The free flow area is decreased due to the presence of liquid film on the pipe wall. Thus, the area available for flow of the gas core is

$$A_c = \frac{\pi (D - 2\delta)^2}{4} \qquad (61)$$

where δ is the annular film thickness.

The mixture mass flow rate in the gas core is given by:

$$M_{1g} = M_{en} + M_g = F_e M_{t1} + M_g \qquad (62)$$

The core mixture velocity is defined by as

$$V_m = \frac{M_{1g}}{\rho_m A_c} \qquad (63)$$

Thus, the frictional pressure loss is given by the following equation:

45

$$\frac{dp}{dz}_f = \frac{\rho_m f_t V_m^2}{2D} \tag{64}$$

where the friction factor, f_t, is defined by the modified

Zigrang-Sylvester equation [62]:

$$\frac{1}{\sqrt{f_d}} = -2.0 \log \left\{ \frac{\epsilon/D}{3.7} - \frac{5.02}{N_{Re,m}} \log \left[\frac{\epsilon/D}{3.7} - \frac{5.02}{N_{Re,m}} \right] \right\} \tag{65}$$

The mixture Reynolds number is defined as

$$N_{Re,m} = \frac{D\rho_m V_m}{\mu_m} \tag{66}$$

where

$$\mu_m = \lambda \mu_l + (1-\lambda)\mu_g \tag{67}$$

The relative roughness of the annular liquid film is taken as the ratio of the time average film thickness to the pipe diameter. This is given by

$$\frac{\epsilon}{D} = \frac{\delta}{D} = \frac{6.95F}{(1 + 1400F)^{1/2}} \tag{68}$$

where

$$F = \frac{\{[0.707(N_{Re,l})^{0.5}]^{2.5} + [0.0379(N_{Re,g})^{0.9}]^{2.5}\}^{0.4}}{(N_{Re,g})^{0.9}(\mu_g/\mu_l)(\rho_l/\rho_g)^{0.5}} \tag{69}$$

and

$$N_{Re,l} = \frac{4M_{lf}}{\mu_l D} \tag{70}$$

$$N_{Re,g} = \frac{\rho_g D V_{sg}}{\mu_g} \tag{71}$$

The pressure loss contributions due to elevation and acceleration are given by the conventional equations:

$$\frac{dp}{dz}_E = \rho_m \tag{72}$$

and

$$\frac{dp}{dz}_A = \frac{\rho_m V_m dV_m}{dz} \tag{73}$$

Thus, the total pressure loss over an increment of length z is expressed as

$$\frac{dp}{dz} = \frac{\rho_m f_t V_m^2}{2D} + \rho_m + \frac{\rho_m V_m dV_m}{dz} \tag{74}$$

The relationship between the above equations is very complex. The quantity of liquid entrained in the gas core depends on the thermodynamic and physical properties of the fluid, as well as the flow rate and channel geometry. The extent of mist entrainment determines the free area available for flow through the channel, and thus directly affects the pressure drop. These complex interrelationships are shown in Figure 6.

47
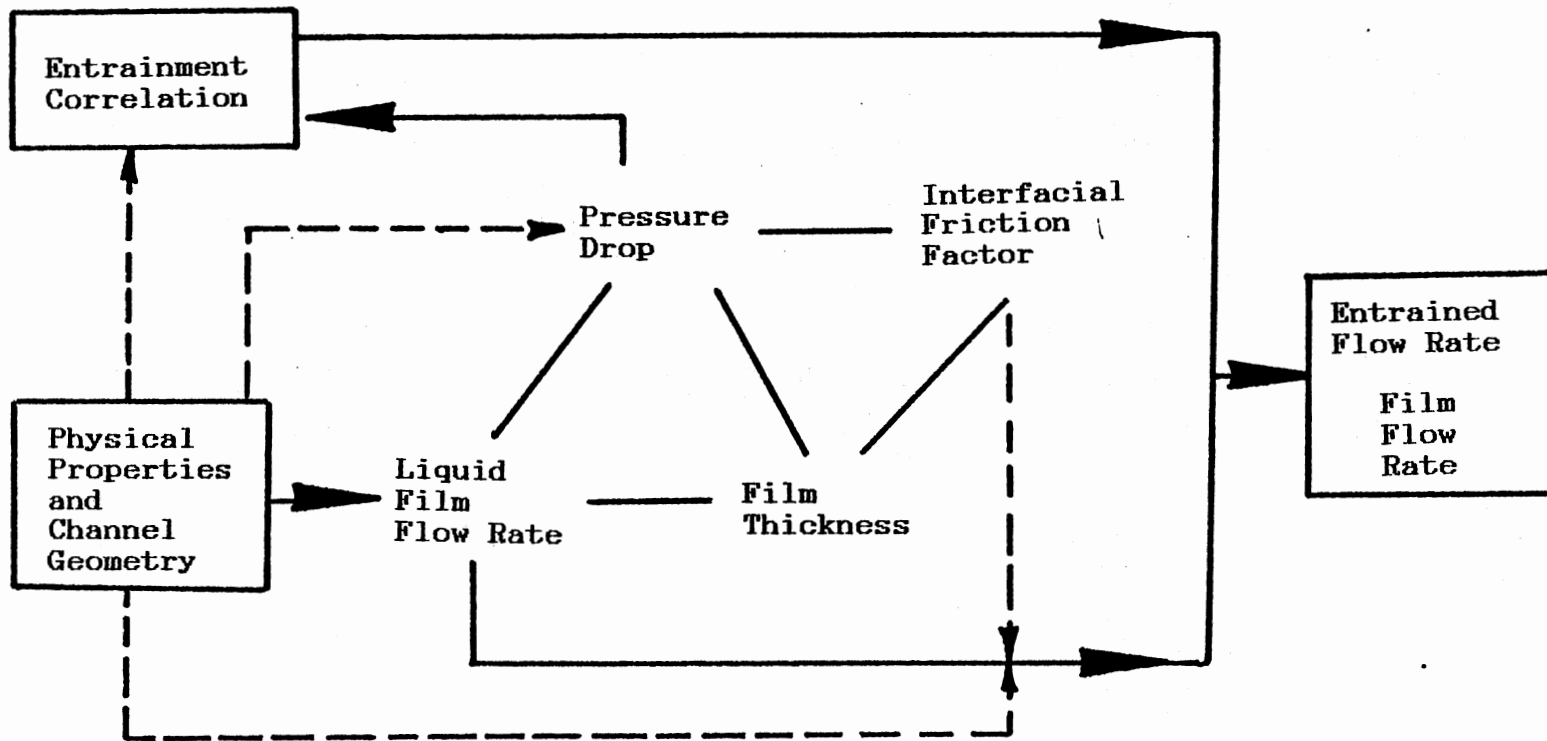
Figure 6.   Inter-relationships For Pressure Loss Calculation
In Annular-Mist Flow   (After Collier [10]).

Using the DOWN*HOLE Program

Introduction

This section of the text is designed to provide the reader with an overview of the program, outline the most efficient method of using the system, point out potential execution problems, and describe novel uses of the simulator.

Model Structure

The DOWN*HOLE model is structured so as to provide easy manipulation of well parameters during operation. In addition, output files may be created by the user during program execution. A flow chart of the model structure is shown in Figure 7. Input and output options are provided, as well as six working options. The Master Menu (see Table I) allows the user to select the desired run option after each section of the program is executed, subject to certain limitations (described below).

The program is executed with a series of 2- and 4-letter mnemonic commands. Four letter commands are exclusively reserved for Master Menu commands. Two letter mnemonic commands are used at all other prompts in the system. Table II describes the 2 letter commands used in the program.
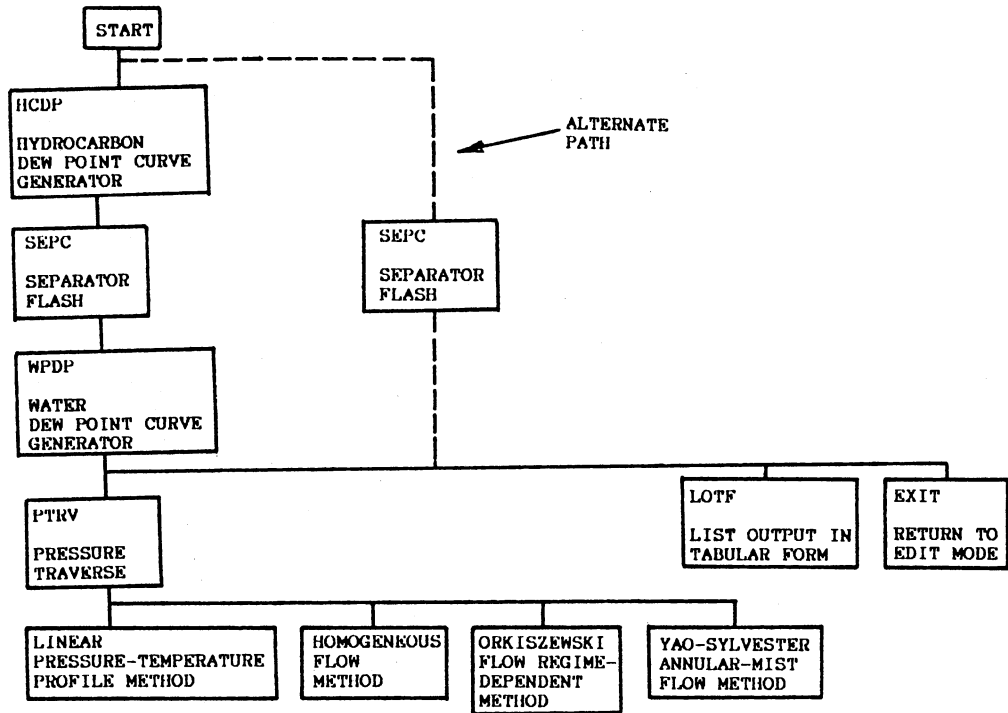
Figure 7.   Flow Chart Of The DOWN*HOLE Production
String Simulation Program.

TABLE I

MASTER MENU COMMAND LIST

Command	Description
HCDP	generates data for HydroCarbon DewPoint curve
WPDP	generates data for Water Phase DewPoint curve
SEPC	calculates flash using SEParator Conditions
BHFW	determines BottomHole Free Water using given conditions
WHFW	determines WellHead Free Water using given conditions
PTRV	determines Pressure TRaVerse throughout production string using selected two-phase flow pressure drop method
LOTF	Lists Output in Tabular Form
EXIT	EXIT's main menu to edit mode

51

TABLE II

EDIT COMMAND SUMMARY

Command		Description
MM		Returns program execution to the Main Menu. The user will then be asked to enter a new four letter master command.
BH		Requests new values for BottomHole temperature and pressure.
WH		Requests new values for WellHead temperature and pressure.
SC		Requests new values for Separator Conditions (operating temperature and pressure).
PR_	*	Changes the print option. When 1 is entered, the long output is selected. Option 2 is for the abbreviated output.
FD_,1	*	Changes the feed rate of a desired component.
RN	*	Runs the current selection from the edit mode.
PP1	*	Changes the initial pressure guess.
TT1	*	Changes the initial temperature guess.
NW		Requests a new problem definition. CAUTION: Information from previous calculations are not erased.
DN	*	Terminates program execution.

* Denotes original GPA*SIM Edit Command

52

Description of Options

Input

The input option is an option which is not user executable. It is automatically initiated when the program is first started or when a new problem is requested. The input section consists of administrative and calculational segments.

Administrative Input. This section of the input subroutine requests from the user information such as the date, user's name, the company and division for which the work is being done, the name of the person requesting the work, charge number, and the well name. After entering this information, it is echo printed on the screen and the user if asked if the information is correct. If the information is incorrect, the sequence is repeated. If the user responds that the information is correct, the calculational input subroutine is called.

Calculational Input. This segment of the program begins with a request for the temperature and pressure at the separator, bottomhole, and wellhead. The user is asked if the information is correct; if it is not, the sequence is repeated; if it is, the user is given the option to create plotting files containing wellhead and bottomhole conditions. After the user has completed the file creation task, the Master Menu appears and prompts

53

for the first working option. The user must select the
hydrocarbon-rich phase dewpoint curve generator (HCDP) as
the first option.

After the first working option is selected, the user
is asked to enter the number of hypothetical undefined
heavy oil components in the produced fluid. Upon satis-
fying this request, the component menu is displayed on
the screen. Figure 8 is the component menu as it appears
to the user. A complete list of compounds common to the
gas processing industry, and available in DOWN*HOLE, is
listed in Table III.

The user is now asked to enter the component identi-
fication number and daily molar flow rate for each
component in the produced fluid. Each organic and
inorganic compound (with the exception of water) should
be entered in order of relative volatility. Entering
components in this order allows the user to check the
trend of component K-values as calculations proceed. The
last component entered should be water. Water should be
entered with a flow rate of zero if the HCDP option was
selected above. Component input is terminated by
entering 0,0 at the next component request. Program
execution will proceed with the working option selected
at the Master Menu (HCDP).

COMPONENT MENU

The Following Components are Most Commonly Used

See Users Manual for a Complete Component List

ID NO.	COMPONENT NAME	ABBREVIATION
2	METHANE	CH4
3	ETHANE	C2H6
4	PROPANE	C3H8
5	ISO-BUTANE	I-C4H10
6	N-BUTANE	N-C4H10
7	ISO-PENTANE	I-C5H12
46	NITROGEN	N2
47	OXYGEN	O2
49	CARBON DIOXIDE	CO2
50	HYDROGEN SULFIDE	H2S
61	WATER	H2O
62+	HYPO COMP'S.	USER SPECIFIED

Figure 8.   Component Menu In The DOWN*HOLE Production
String Simulation Program.

TABLE III

LIST OF COMPONENTS USED IN DOWN*HOLE

Component No.	Name	Program Symbol
1	Hydrogen	H2
2	Methane	CH4
3	Ethane	C2H6
4	Propane	C3H8
5	iso-Butane	I-C4H10
6	n-Butane	N-C4H10
7	iso-Pentane	I-C5H12
8	n-Pentane	N-C5H12
9	neo-Pentane	NEO-C5
10	n-Hexane	N-C6H14
11	n-Heptane	N-C7H16
12	n-Octane	N-C8H18
13	n-Nonane	N-C9H20
14	n-Decane	N-C10H22
15	n-Undecane	N-C11H24
16	n-Dodecane	N-C12H26
17	n-Tridecane	N--C13H28
18	n-Tetradecane	N-C14H30
19	n-Pentadecane	N-C15H32
20	n-Hexadecane	N-C16H34
21	n-Heptadecane	N-C17H36
22	Ethylene	C2H4
23	Propylene	C3H6=
24	1-Butene	1-C4H8
25	cis-2-Butene	C-2-C4H8
26	trans-2-Butene	T-2-C4H8
27	iso-Butene	I-C4H8
28	1,3 Butadiene	1,3-C4==
29	1-Pentene	1-C5H10

TABLE III (Continued)

Component No.	Name	Program Symbol
30	cis-2-Pentene	C-2-C5=
31	trans-2-Pentene	T-2-C5=
32	2-Methyl-1-Butene	2MT-1C4=
33	3-Methyl-1-Butene	3MT-1C4=
34	2-Methyl-2-Butene	2MT-2C4=
35	1-Hexene	C6H12=
36	Cyclopentane	CYC-C5
37	Methylcyclopentane	MTCYC-C5
38	Cyclohexane	CYC-C6
39	Methylcyclohexane	MTCYC-C6
40	Benzene	BZ
41	Toluene	TOL
42	o-Xylene	O-X
43	m-Xylene	M-X
44	p-Xylene	P-X
45	Ethylbenzene	EB
46	Nitrogen	N2
47	Oxygen	O2
48	Carbon Monoxide	CO
49	Carbon Dioxide	CO2
50	Hydrogen Sulfide	H2S
51	Sulfur Dioxide	SO2
52	2-Methyl-Pentane	2-MT-C5
53	3-Methyl-Pentane	3-MT-C5
54	2,2 Dimethyl-Butane	2,2 DMTC4
55	2,3 Dimethyl-Butane	2,3 DMTC4
56	1-Heptene	1-C7H14=
57	Propadiene	C3H4==
58	1,2 Butadiene	1,2-C4==
59	Ethylcyclopentane	ETCYC-C5
60	Ethylcyclohexane	ETCYC-C6
61	Water	H2O
>62	Hypothetical	User Specified

Hydrocarbon-Rich Phase Dew Point Curve
Generator (HCDP)

The HCDP working option is a user-executable command which generates and stores pressure-temperature data in the file HCDP.DAT. The program generates a curve from 100 psia to near the critical pressure of the system. As stated earlier, this option must be the first selected at the Master Menu. This inconvenience is due to the structure of the GPA*SIM program, about which DOWN*HOLE is built.

The hydrocarbon-rich phase dew point curve is generated within the existing structure of GPA*SIM. The GPA*SIM edit command OP3 is used to perform temperature-dependent dew point calculations. Starting pressure, ending pressure, and pressure increments (GPA*SIM edit commands PP1, PP2, and PP3) are internally set at 90, 3500, and 10 psi, respectively. In addition, a "reasonable" first guess for a starting temperature is needed to sucessfully begin creating the curve. This value is internally set at -60° F, and has worked without failure in all cases tested in this project.

The internal starting pressure of 90 psia is an arbitrary starting point at the lowest conceivable useful pressure of interest to the user. The 3500 psia ending pressure exceeds the critical pressure of most hydrocarbon mixtures of interest, thus the curve may be generated up to (or near) the system cricondenbar. Finally, the pressure increment is set at 10 psi for the purpose of avoiding convergence problems in GPA*SIM. Use of such a small

58

pressure increment allows the program to "crawl" up the dew point curve past the cricondentherm, where most convergence problems occur when using large pressure increments. Figure 9 is a flowchart of the hydrocarbon phase dew point curve generator.
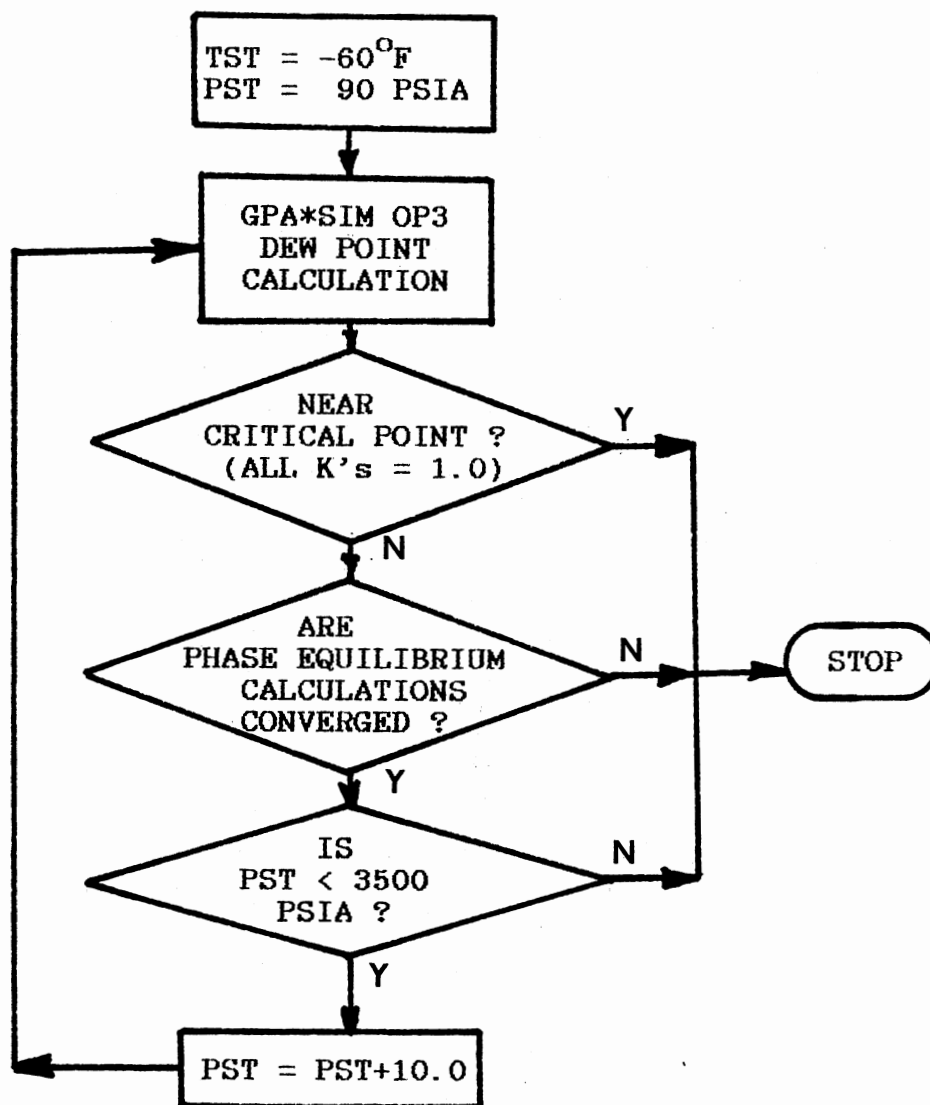
Separator Flash Option (SEPC)

The SEPC command is provided primarily as a method to account for water in the gas phase. Typical gas analyses do not specify the amount of water in the gas. Thus, SEPC allows the user to change the amount of water in the feed until the measured quantity of liquid water is produced at separator conditions.

Water-Rich Phase Dew Point Curve Generator (WPDP)

This command generates pressure-temperature data for the water phase dewpoint curve. Eleven data points are generated from 100 psia to 3400 psia. The data are automatically stored in an internal file called WATER.DAT. This option should be used only after the correct quantity of water has been established with the SEPC command.

The water dew point curve is generated by performing flash calculations at selected points of specified temperature and pressure. The starting pressure and temperature are set at 100 psia and $200^{O}F$ respectively. While the pressure remains constant the temperature is

59

TST = -60°F
PST = 90 PSIA

GPA*SIM OP3
DEW POINT
CALCULATION

NEAR
CRITICAL POINT ?
(ALL K's = 1.0)   Y

N

ARE
PHASE EQUILIBRIUM
CALCULATIONS
CONVERGED ?   N

STOP

Y

IS
PST < 3500
PSIA ?   N

Y

PST = PST+10.0

TST = TEMPERATURE
PST = PRESSURE

Figure 9.   Flowchart For Generating The Hydrocarbon
Phase Dew Point Curve.

reduced in increments of 10^OF until water condenses. The temperature is then increased by 5^OF until liquid water is no longer present. Finally, the temperature is reduced by 1^OF increments until water condenses again. This is taken as the water dew point. The procedure is repeated at 300 psi increments up to 3400 psia. Figure 10 is a flowchart of this procedure.

### B.3.5. Wellhead Flash (WHFW)

The WHFW command is provided so the user may determine whether free liquid water is present at wellhead conditions. Running this option is not necessary because all information generated here is available from the Pressure Traverse option.

Bottomhole Flash (BHFW)

The BHFW option is provided so the user may determine whether free liquid water is present at bottomhole conditions. As with the WHFW command, BHFW does not need to be run because all information generated here is available from the Pressure Traverse option.

Pressure Traverse Generator (PTRV)

Selecting the PTRV command gives the user the option of generating a well pressure traverse with one of four options. Invoking the PTRV command causes the Pressure Traverse Menu to be displayed (See Figure 11). When the
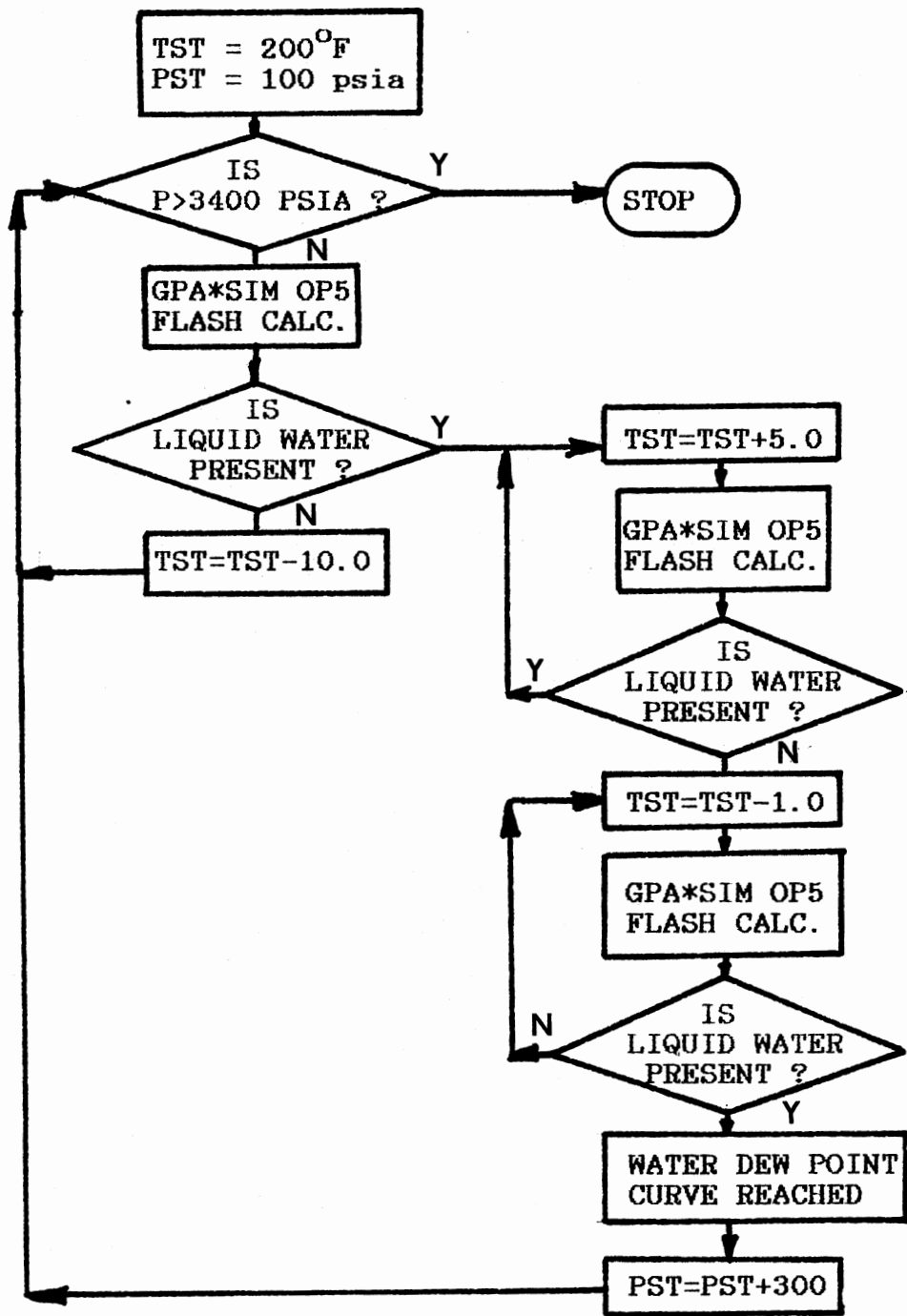
TST = TEMPERATURE
PST = PRESSURE

Figure 10.   Flowchart For Generating The Water
Phase Dew Point Curve.

You have the choice of 4 pressure drop
correlations:

1 = Assume a linear Pressure-Temperature Profile

2 = Homogeneous Flow Model, Enthalpy Specified

3 = Homogeneous Flow Model, Temperature Specified

4 = Orkiszewski Flow Model, Enthalpy Specified

5 = Orkiszewski Flow Model, Temperature Specified

6 = Annular-Mist Flow Model, Enthalpy Specified

7 = Annular-Mist Flow Model, Temperature Specified

8 = EXIT TO MASTER MENU

Enter your choice of options: 1

Figure 11.   Pressure Traverse Menu In The DOWN*HOLE
Production String Simulation Program.

user selects one of the eight executable options, prompts are made for string geometry parameters and the heat loss factor.

The pressure traverse is created by starting at the bottomhole of the hole with the a calculation. Physical properties at bottomhole conditions are used to calculate the pressure drop over the first increment of the procuction string. A new average pressure for the increment is calculated, and physical properties are obtained by flashing the produced fluid at the average temperature and pressure of the increment. This procedure is repeated until the average pressure of the increment converges to within 0.01 psi.

String Geometry Input Section.

This section of the program is automatically invoked when the first Pressure Traverse selection is made. The user is asked to enter the total length of the production string, and the number of different sizes of tubing in the hole. The program then prompts the user for the diameter and depth of the top of each different size of tubing. Finally, the user is asked to enter the increment length used in the pressure drop calculation. This length should be between 150 and 600 ft. Using a length shorter than 150 ft. can result in exceptionally long execution time, while using a length greater than 600 ft. may generate output of questionable accuracy.

All of the string parameters are echo printed to the

64

screen, and the user is asked to make any necessary corrections. If there is any incorrect information, the input section is repeated.

Specifying the Fluid Enthalpy Profile. After correct string geometry parameters have been entered, DOWN*HOLE performs flash calculations at specified wellhead and bottomhole conditions. The fluid enthalpy difference between the bottom of the hole and wellhead is calculated, and the heat loss per foot of tubing is determined. The key assumption in this program is that the fluid enthalpy is approximated as a linear function of depth.

The program next displays the heat loss per foot of tubing per unit time and prompts the user for a heat loss factor. The heat loss factor represents the fraction of the linear enthalpy difference which is to be used in the pressure loss calculation. Note that the heat loss factor is used only in PTRV options 2, 4, and 6. The heat loss factor has no effect on PTRV options 1, 3, 5, and 7; thus, any value may be entered when using these options.

If the user specifies a heat loss factor of unity, this implies a linear fluid enthalpy decrease with depth from known bottomhole conditions to known wellhead conditions. A heat loss factor less than unity implies that the fluid enthalpy will decrease at a greater rate up the string than would result if a unity heat loss factor were used. By the same token, a heat loss factor greater than unity results in the fluid enthalpy decreasing at a slower rate up the string

than the factor of one.

Simulating the Production String.   Downhole
conditions are modeled by performing sequential three-phase
temperature or enthalpy dependent flash calculations upward
from the bottom of the well.   Pressure Traverse options 2,
4, and 6 specify the fluid enthalpy profile via the heat
loss factor method outlined previously.   Options 3, 5, and 7
utilize a linear temperature profile throughout the well.
In both categories of calculations, the pressure is set by
an iterative algorithm between the desired pressure drop
correlation and the phase equilibrium package.

The linear pressure-temperature profile option (PTRV
option 1) does not perform pressure drop calculations.   The
subroutine performs enthalpy-dependent flash calculations at
a user-specified number of points in the production tubing.
Based on the assumptions of both the linear pressure and
temperature profiles, mass fractions of gas, oil, and water
are determined at the selected locations.

The Homogeneous, Orkiszewski, and Yao-Sylvester flow
methods simulate the production string using the iterative
procedure described above.   These correlations are also
modified to determine local fluid velocities at several
points in the string.   In addition, the erosional velocity
is calculated using a method developed by the American
Petroleum Institute.

The API has developed a system for determining the
maximum recommended fluid velocity in flow lines [3].   In

66

order to prevent erosion due to fluid impingement,
Recommended Practice 14E predicts the erosional velocity
from the following equation:

$$V_e = \frac{C}{\rho_m^{1/2}} \qquad (75)$$

where

V_e = fluid erosional velocity, ft./sec.

C = 100; an empirical constant, and

ρ_m = gas/liquid mixture density, lb./cu. ft.

API RP-14E is not designed for application to tubular
goods. However, application (or misapplication) to downhole
situations is not uncommon.

The user is given the opportunity to print a hard copy
of the generated data at the end of each pressure traverse
simulation. This intermediate output need not be generated,
as the last run from each PTRV option is saved in a master
array, accessible with the LOTF command.

The user is now given the option to create the following
plotting files:

Well Pressure-Temperature Path

Temperature-Depth Profile

Pressure-Depth Profile

Actual Velocity-Depth Profile

Erosional Velocity-Depth Profile

Finally, the program gives the user an opportunity to

re-run the current pressure traverse option. If the current option is to be run again, the string geometry parameters and heat loss factor are echo printed, and the opportunity to make modifications is given. If the user wishes to run another pressure traverse option, the Pressure Traverse Menu is displayed. When the desired correlation is selected, string geometry parameters are echo printed, then execution proceeds.

Tabular Output List Option (LOTF)

This command is set up to create tables of data generated in the PTRV section of the program. Administrative information, separator, wellhead, and bottomhole conditions, and the most recent set of data from each pressure traverse option are output. This command may be accessed from the Master Menu at any time during program execution.

Exit Master Menu (EXIT)

The EXIT command is set up to transfer program execution to the edit mode.

CHAPTER V

ERROR ANALYSIS

Introduction

This chapter presents an in-depth error analysis of
the Pressure Traverse section of the DOWN*HOLE computer
program. The primary purpose of this program is to
accurately predict the location of the water condensation
zone in the production tubing of gas wells. Unfortunately,
information in the literature pertaining to the location of
the water-wet zone is non-existent. Thus, two key
assumptions must be made. First, the assumed linear
temperature profile is taken as correct. Secondly, the
accuracy of the pressure drop correlations is assumed to
reflect directly on the ability of the program to predict
conditions in the water-wet zone. Thus, the information
presented here analyzes the accuracy of the pressure drop
correlations.

It should be noted that only the specified temperature
profile options are analyzed here. Enthalpy profile speci-
fied options 2, 4, and 6 were found to produce extremely
large errors. Furthermore, these options also introduced a
significant error component into the predicted wellhead

temperature. Thus, the assumption of the linear fluid enthalpy profile between bottomhole and wellhead conditions is deemed inappropriate for the cases presented here. All cases were run assuming a 500 ft. long calculation increment. All data used in and generated by this work may be found in the DOWN*HOLE Program Supplement [20].

Data Analysis

The DOWN*HOLE Production String Simulation Package requires accurate fluid composition data to perform properly. That is, more information is needed than simply gas gravity data. A detailed gas analysis, such as those frequently performed when a well is put on production, is required. The literature revealed no detailed information of this type. However, one source was uncovered which provided gas gravity data along with substantial qualitative information about the gas composition. This source provided 70 case histories from 26 producing wells. The data were obtained from production tests and production control surveys. The range of the test data is presented in Table IV.

Composition Data

The data taken from Reinicke et al. [48] show the wells produce a dry sweet gas with a density of 0.63 to 0.80 relative to air. The combustible fraction of the gas

70

TABLE IV

RANGE OF TEST DATA

	Minimum	Maximum
Depth (Ft.)	10082	16207
Gas Gravity (Air = 1.0)	0.63	0.80
Gas Flow Rate (MMSCFD)	0.40	44.9
Water/Gas Ratio (BBL/MMSCF)	0.70	132
Bottomhole Pressure (PSIA)	2335	8905
Wellhead Pressure (PSIA)	1175	6991
Bottomhole Temperature (^{O}F)	214	315
Wellhead Temperature (^{O}F)	59	223

contains mainly methane with very little heavy hydrocarbons (C_{4+} < 0.05 volume %). The higher gas gravities are due to the presence of nitrogen in the gas, as much as 50 mol % in some cases. The quantity of other non-hydrocarbon gases is negligible.

Using this information in concert with personal experience led to the development of typical gas composit- ions used to test the DOWN*HOLE program. The five gas compositions used in the simulations are shown in Table V.

Pressure Drop Statistics

The Homogeneous Flow, Orkiszewski, and Yao-Sylvester pressure loss prediction methods were tested using the DOWN*HOLE simulation package. The predicted pressure drops were then compared with measured field data. The percent error was plotted against the water/gas ratio. A brief summary of the statistical results obtained from the program test is presented in Table VI.

The definition of percent error, E, mean percent error, $\overline{E}$, and standard deviation of percent error from the mean percent error, D_s, are given by

$$E = \frac{\Delta p_c - \Delta p_m}{\Delta p_m} \times 100 \tag{76}$$

$$\overline{E} = \frac{1}{n} \sum_{i=1}^{n} E_i \tag{77}$$

and

TABLE V

GAS COMPOSITIONS USED IN PROGRAM TEST

Gas Gravity	Composition
0.80	N_2 = 48.81% C_1 = 43.69% C_2 = 6.00% C_3 = 1.50%
0.79	N_2 = 45.41% C_1 = 45.99% C_2 = 7.20% C_3 = 1.40%
0.65	C_1 = 85.40% C_2 = 9.80% C_3 = 4.80%
0.64	C_1 = 87.30% C_2 = 8.10% C_3 = 4.60%
0.63	C_1 = 87.60% C_2 = 9.55% C_3 = 2.85%

TABLE VI

DATA SUMMARY

Flow Correlation	Comments
Homogeneous Flow Method	29 cases failed to converge 41 cases converged Overall Avg. Error = 101.4% Error Range: 33.5 – 276.2% 0 cases under-predicted pressure drop
Orkiszewski Flow Method	11 cases failed to converge 59 cases converged Overall Avg. Error = 44.9% Error Range: –23.7 – 139.6% 5 cases under-predicted pressure drop
Yao Flow Method	9 cases failed to converge 61 cases converged Overall Avg. Error = 24.8% Error Range: –55.1 – 252.6% 23 cases under-predicted pressure drop

Basis: 70 case histories from 26 gas wells
        14 cases produced only condensed water

$$D_s = \sqrt{\frac{1}{(n-1)} \sum_{i=1}^{n} (E_i - E)^2} \qquad (78)$$

where

Δp_c calculated pressure difference,

Δp_m measured pressure difference, and

n number of wells in the test group.

The percent error, E, as defined in equation (76), may be any positive number, but is bounded on the low side by -100%. This definition of error tends to over emphasize overpredicted pressure losses. By the same token, the standard deviation emphasizes the scatter of overpredicted pressure losses. The significance of the error for the cases where pressure drop is underpredicted should not be underestimated. Percent error data for each flow correlation are given in Figures 12, 13, and 14.

The error data have been grouped into seven distinct classes, according to the produced water/gas ratio. The data are classified so that any potential user of the program may estimate the expected error magnitude. Table VII presents the grouped data, along with the number of data points for each class and the mean percent error of each pressure loss method. Figure 15 is a plot of the mean percent error for each group of data. Figure 16 presents the standard deviation of the grouped data.
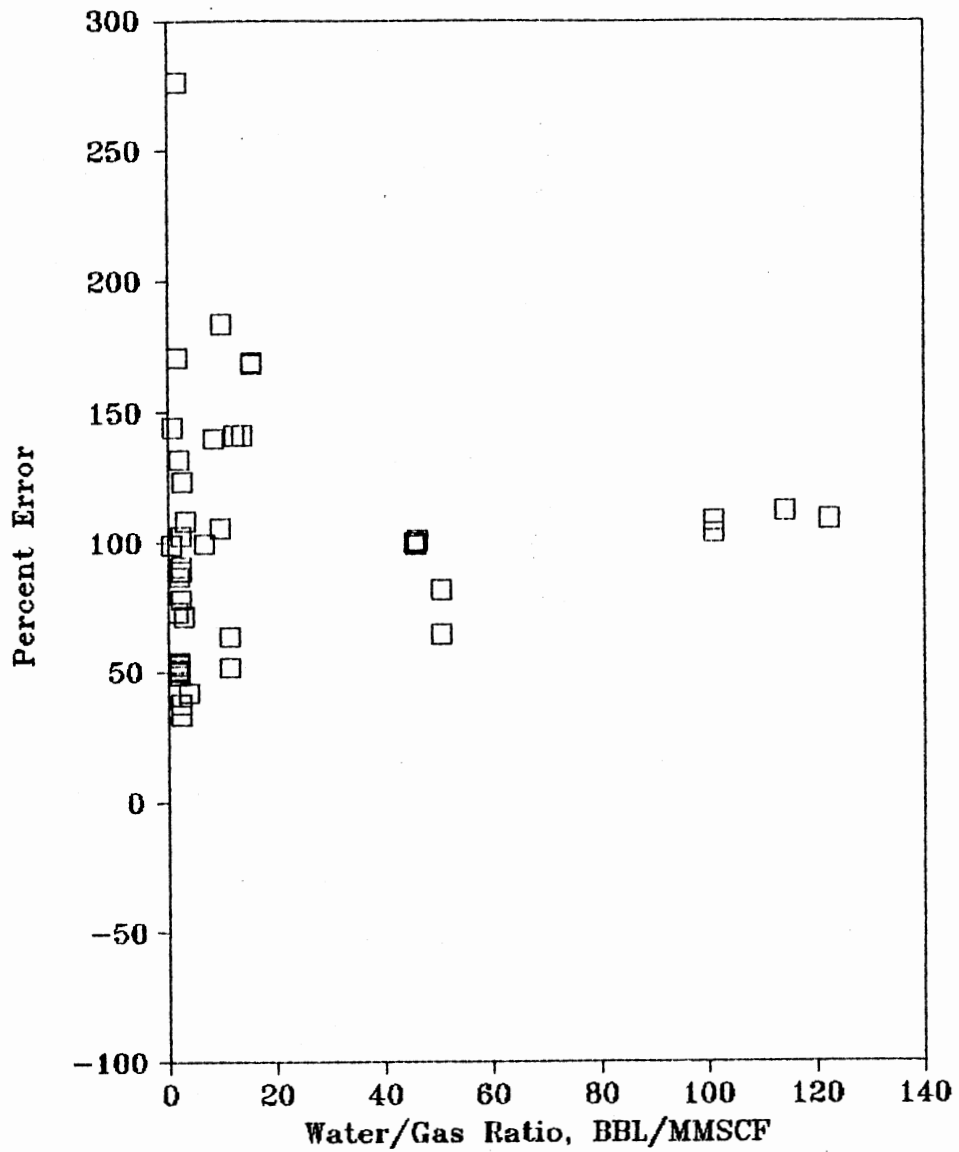
Figure 12.   Percent Error For Each Data Point
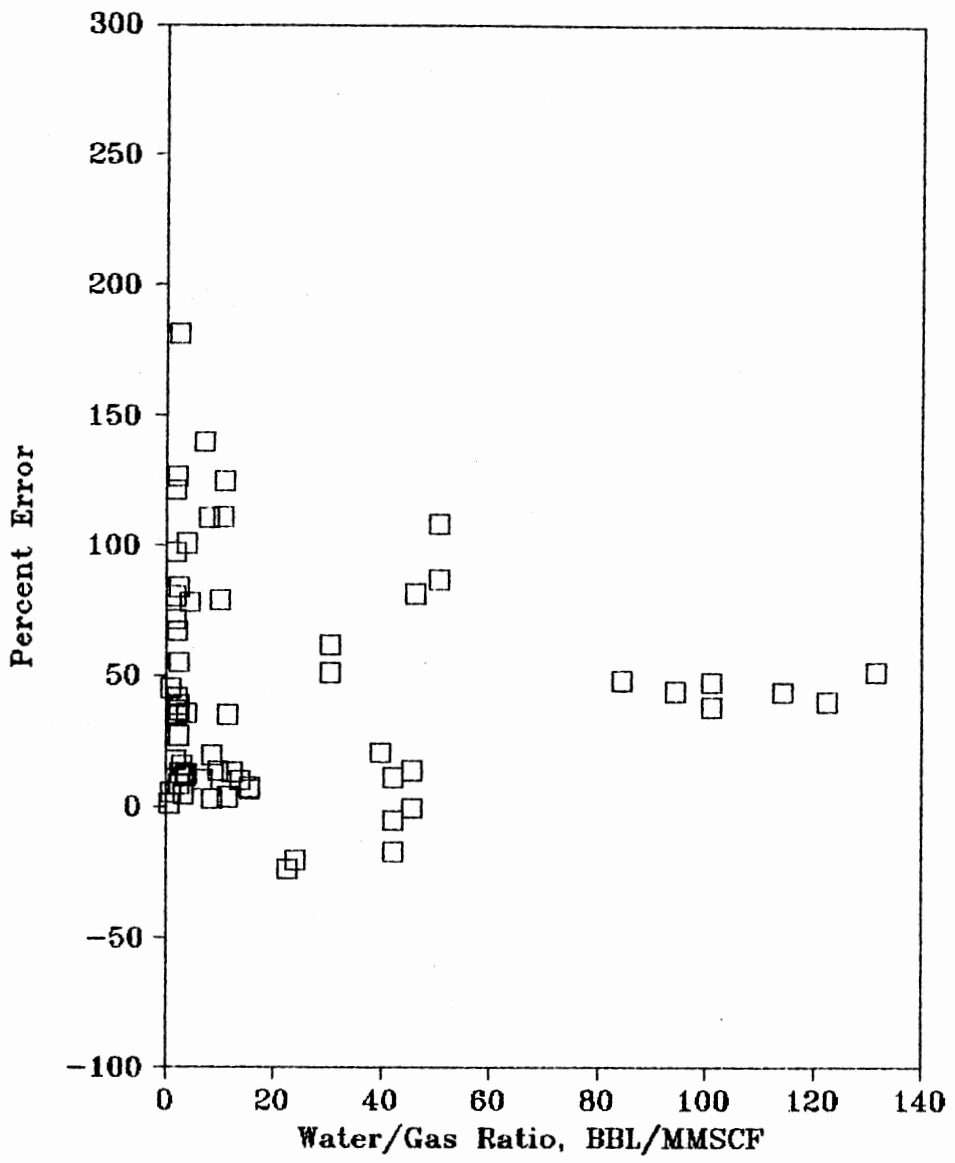   Homogeneous Flow Correlation.

Figure 13.   Percent Error For Each Data Point
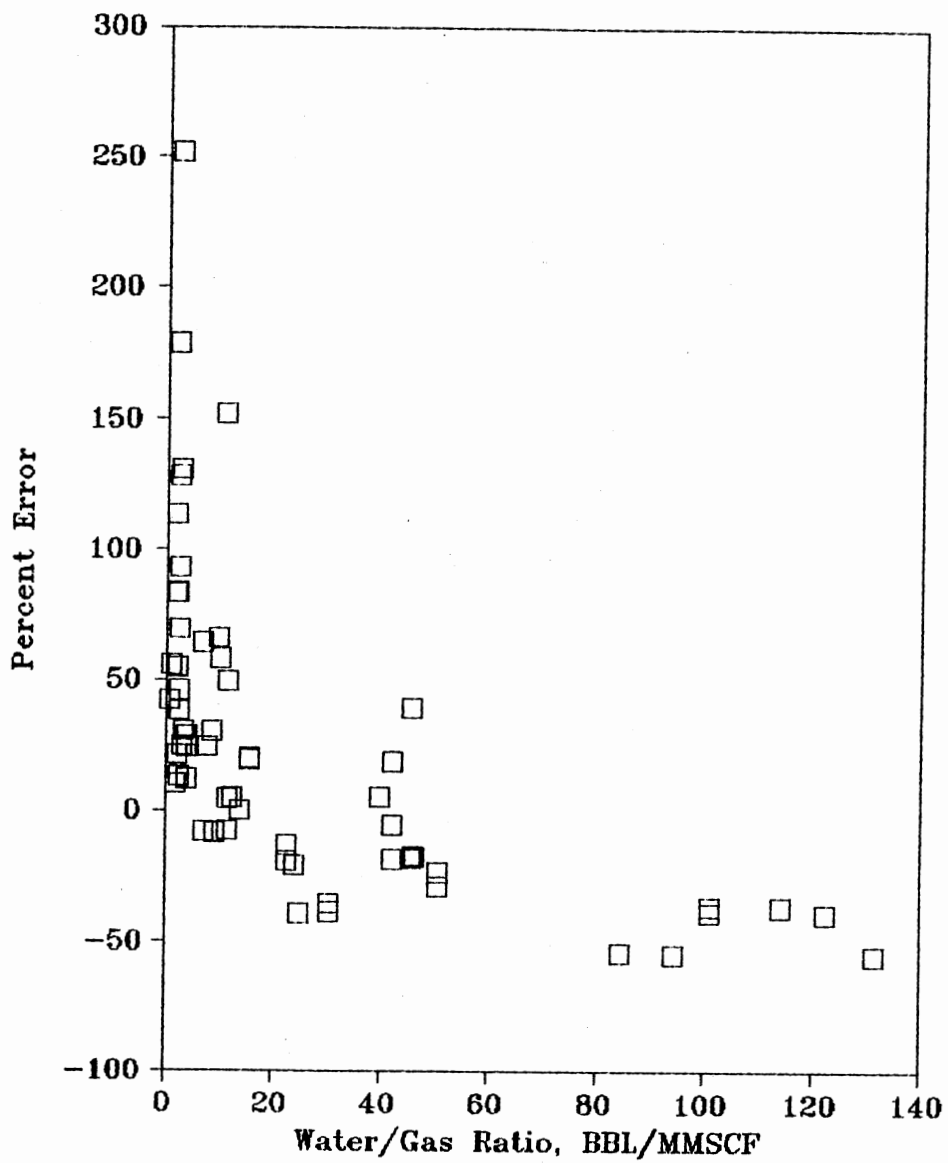Orkiszewski Flow Correlation.

Figure 14.   Percent Error For Each Data Point
Yao-Sylvester Flow Correlation.

TABLE VII

SUMMARY OF GROUPED DATA

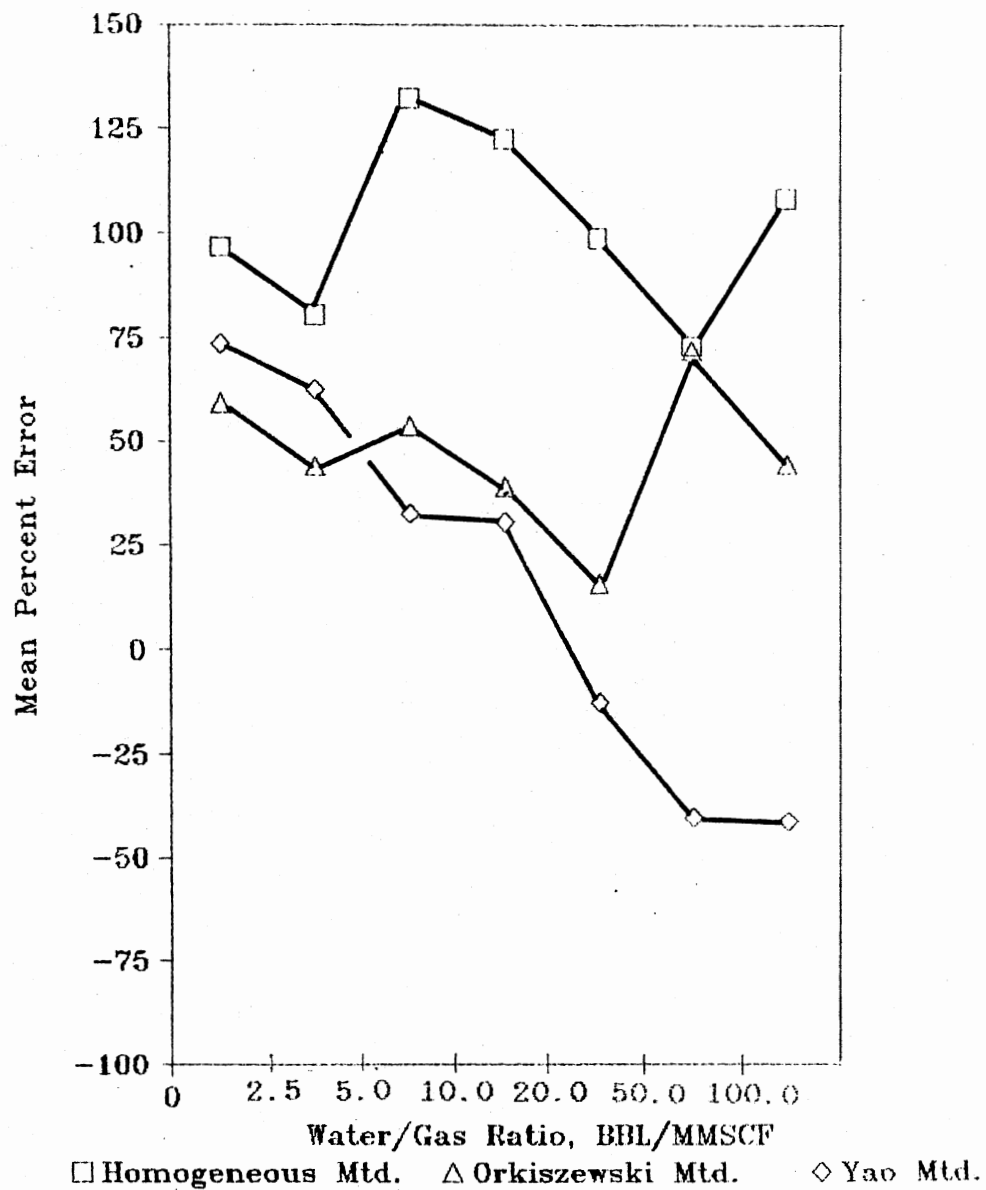| Class (BBL/MMSCF)	Number of Points			Mean Percent Error		
	Homg.	Ork.	Yao.	Homg.	Ork.	Yao.
0 to 2.5	15	15	14	97.8	59.1	73.5
2.5 to 5.0	7	12	9	80.5	44.0	62.5
5.0 to 10.0	4	7	7	132.2	53.7	32.5
10.0 to 20.0	6	8	8	122.6	39.0	30.5
20.0 to 50.0	3	9	14	99.8	5.5	−12.8
50.0 to 100.0	2	3	4	73.0	79.8	−40.3
100.0 +	4	5	5	108.2	44.3	−41.3

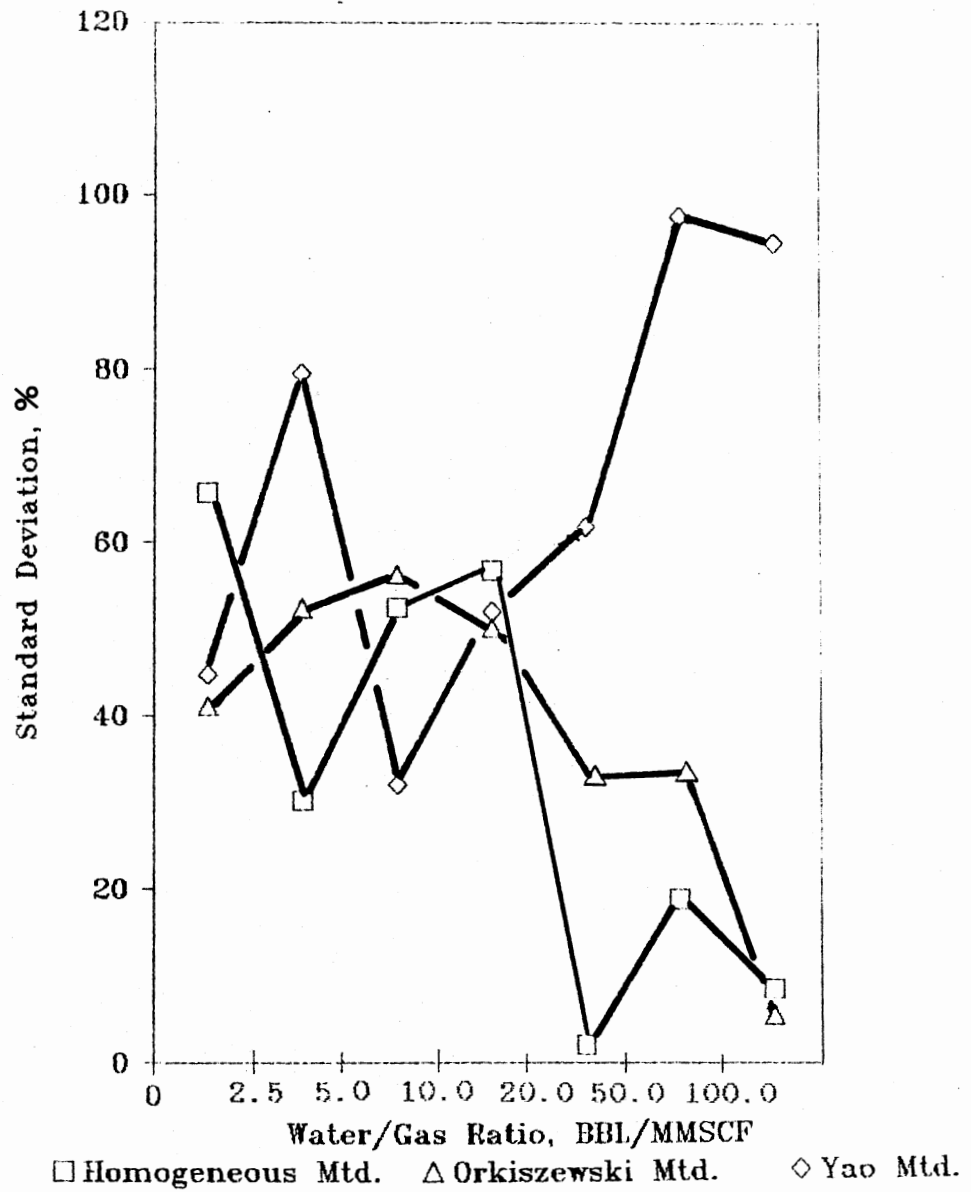Figure 15.   Mean Percent Error For All Flow
Correlations.

Figure 16. Standard Deviation About Mean Percent Error For All Flow Correlations.

Discussion of Results

Figures 12 through 16 reveal the test data are quite scattered. This is to be expected given the current state of predicting two-phase pressure drop. Pressure loss was calculated from the bottom of the well to the wellhead. The pressure was bounded by zero at the wellhead. In some instances, the calculated pressure was predicted as zero (or less) before the wellhead was reached. Such data points are not included in the statistical analysis. The Yao-Sylvester flow correlation failed to converge in some cases. Again, these results are not included in the data analysis.

In general, the poor accuracy exhibited in these results is attributed to the pressure drop prediction methods. The current state-of-the-art for predicting pressure losses in two-phase flow leaves much to be desired. The phase equilibrium package performed admirably and never failed to converge.

Homogeneous Flow Method

The Homogeneous Flow Method produced surprisingly poor results. The correlation overpredicted pressure drop in all cases. The method was expected to produce reasonable results for those wells with a low water/gas ratio. This was not the case. In most cases, the quantity of condensed water near the top of the string produced larger than expected pressure losses. This error was compounded as the

82

calculation neared the top of the string.

Orkiszewski Flow Method

The Orkiszewski Flow Method produced the best results
of the three methods tested. Although this correlation
consistently overpredicted the pressure drop, it performed
better than the Homogeneous Method. The reader should
realize that the data were scattered, and in some cases,
the correlation will produce totally unacceptable results.

Yao-Sylvester Flow Method

The Yao-Sylvester Flow Method consistently under-
predicted the pressure drop for wells with a producing
water/gas ratio of greater than 15 bbl/MMscf. Because the
error analysis tends to under-emphasize under-predicted
pressure losses, this method should be used with caution.
Many times this correlation failed to correctly predict the
fraction of liquid entrained in the gas core. This is
probably due to the fact that the correlation used to
estimate the wall film thickness failed. This failure was
caused by the extremely high Reynolds numbers encountered
in the test wells [31].

As previously stated, the underprediction of pressure
drop generally occurred in the high water cut wells. Many
of these wells may not be flowing in the annular mist
regime, thus only the gas density is taken into account in
the head loss term.

CHAPTER VI

CONCLUSIONS AND RECOMMENDATIONS

The purpose of this study was to develop an easy-to-use computer model to predict the location of the water condensation zone in gas wells. DOWN*HOLE is designed to estimate the location of the water-wet zone and, if desired, predict the prevailing flow regime. In addition, the quantity of acid gases dissolved in the water phase may be accurately estimated.

In this work, 70 cases have been run on the simulator. From this experience, the following recommendations can be made:

1. The Orkiszewski flow correlation appears to work best for the cases tested. This may not be the case for all wells, hence all three flow methods should be used when modelling a well.

2. The large scatter of the data underscores the need for more work in the development of two-phase flow pressure drop correlations.

3. The accuracy of the three flow methods included here is questionable. If necessary, other flow correlations should be tested before proceeding to Phase II of the project.

4. The stability of all pressure drop methods may be improved by converting the program from length specification to maximum pressure drop allowed in each increment.

BIBLIOGRAPHY

1) Akashah, S. A., J. H. Erbar, and R. N. Maddox, "Two-Phase Flow Calculations Incorporating an Equation of State," in Proceedings of the Sixty-First Annual Convention, Gas Processors Association, Dallas, Texas (March 15-17, 1982).

2) Aziz, K., G. W. Govier, and M. Forgarsi, "Pressure Drop in Wells Producing Oil and Gas," Journal of Canadian Petroleum Technology, 11(3), 38-42 (July-September 1972).

3) American Petroleum Institute, "Sizing Criteria for Gas/Liquid Two-Phase Lines," Recommended Practice 14E, (August 1975).

4) Baker, O., H. W. Brainerd, C. L. Coldren, Orin Flanigan, and J. K. Welchen, "Gas-Liquid Flow in Pipelines: II. Design Manual," The American Gas Association and The American Petroleum Institute, (October 1970).

5) Baxendell, P. B., "Producing Wells on Casing Flow-An Analysis of Flowing Pressure Gradients," Petroleum Transactions of the AIME, 213, 202-206 (1958).

6) Baxendell, P. B., and R. Thomas, "The Calculation of Pressure Gradients in High-Rate Flowing Wells," Journal of Petroleum Technology, 13(10), 1023-1028 (October 1961).

7) Beggs, H. D., and J. P. Brill, "A Study of Two-Phase Flow in Inclined Pipes," Journal of Petroleum Technology, 25(5), 607-617 (May 1973).

8) Bradburn, J. B., and S. K. Kalra "Corrosion Mitigation - A Critical Facet of Well Completion Design," Journal of Petroleum Technology, 35(10), 1617-1623 (September 1983).

9) Chierici, G. G., G. M. Ciucci, and G. Sclocci, "Two-Phase Vertical Flow in Oil Wells-Prediction of Pressure Drop," Journal of Petroleum Technology, 19(6), 927-938 (June 1967).

10) Collier, John G., "Convective Boiling and Condensation," 2nd. Ed., Chapter 2, McGraw Hill Book Co., London, England (1981).

11) Cornish, R. E., "The Vertical Multiphase Flow of Oil and Gas at High Rates," Journal of Petroleum Technology, 28(7), 825-831 (July 1976).

12) Craig, B., "Critical Velocity Examined for Effects of Erosion-Corrosion," Oil and Gas Journal, 83(14), 99-100 (May 27, 1985).

13) Duns, H., and N. C. J. Ros, "Vertical Flow of Gas and Liquid Mixtures in Wells," in Proceedings of the Sixth World Petroleum Congress, Frankfurt, Germany (June 19-26, 1963).

14) Eaton, Ben A., Donald E. Andrews, Charles R. Knowles, I. H. Silberberg, and Kermit E. Brown, "The Prediction of Flow Patterns, Liquid Holdup and Pressure Losses Occurring During Continuous Two-Phase Flow in Horizontal Pipelines," Journal of Petroleum Technology, 19(6), 815-827 (June 1967).

15) Erbar, John H., "Phillips' Fractionation Workshop," School of Chemical Engineering, Oklahoma State University, Stillwater, Oklahoma (August 1983).

16) Erbar, J. H., "Documentation of the GPA*SIM Program," Gas Processors Association, Tulsa, Oklahoma (August 1980).

17) Erbar, John H., "Three-Phase Equilibrium Calculations," in Proceedings of the Fifty-Second Annual Convention, Gas Processors Association, Dallas, Texas (March 14-16, 1972).

18) Erbar, John H., and Jan Wagner, "Industrial Application of GPA*SIM," in Proceedings of the Sixty-Second Annual Convention, Gas Processors Association, San Francisco, California (March 14-16, 1983).

19) Erbar, R. C., and R. H. Heidersbach, "Computer Simulation for the Prediction of Downhole Corrosion," Engineering Research Proposal No. EN 86-R-108, College of Engineering, Oklahoma State University, Stillwater, Oklahoma (April 18, 1986).

20) Erbar, R. C., and C. A. Robertson, "Data Supplement to the DOWN*HOLE Production String Simulation Package-70 Case Histories," School of Chemical Engineering, Oklahoma State University, Stillwater, Oklahoma (April 1988).

21) Farshad, F. F., J. D. Garber, and J. B. Bradburn, "How to Increase Gas Well Production and Temper Corrosion, Part 1-Production System Optimization," Petroleum Engineer International, $\underline{55}$(4), 82-92 (April 1983).

22) Farshad, F. F., J. D. Garber, and J. B. Bradburn, "How to Increase Gas Well Production and Temper Corrosion, Part 2-Corrosive Variables in a Gas Well," Petroleum Engineer International, $\underline{55}$(5), 84-108 (May 1983).

23) Gas Processors Suppliers Association, "Engineering Data Book," Ninth Edition, Chapter 16, Gas Processors Association, Tulsa, Oklahoma (1972).

24) Gray, H. E., "Vertical Flow Correlation in Gas Wells," API 14B, Appendix B-Section 1, American Petroleum Institute (June 1974).

25) Griffith, Peter, and Graham B. Wallis, "Two-Phase Slug Flow," Journal of Heat Transfer, $\underline{83}$(3) 307-320 (August 1961).

26) Hagedorn, Alton R., and Kermit E. Brown, "Experimental Study of Pressure Gradients Occurring During Continuous Two-Phase Flow in Small Diameter Vertical Conduits," Journal of Petroleum Technology, $\underline{17}$(4), 475-484 (April 1965).

27) Hamby, Tyler W. Jr., "Development of High-Pressure Sour Gas Technology," Journal of Petroleum Technology, $\underline{33}$(5), 792-798 (May 1981).

28) Hamby, T. W., and R. N. Tuttle, "Deep, High-Pressure Sour Gas is Challenge," Oil and Gas Journal, $\underline{73}$(22), 114-120 (May 12, 1975).

29) Hankinson, R. W., T. A. Coker, and G. H. Thomson, "Get Accurate LNG Densities with COSTALD," Hydrocarbon Processing, $\underline{61}$(4), 207-208 (April 1982).

30) Heidersbach, R., "Velocity Limits for Erosion-Corrosion," OTC 4974, Presented at the Seventeenth Annual Offshore Technology Conference, Houston, Texas (May 1985).

31) Henstock, William H., and Thomas J. Hanratty, "The Interfacial Drag and the Height of the Wall Layer in Annular Flows," AICHE Journal, $\underline{22}$(6), 990-999 (November 1976).

32) Hill, A. D., and Donald C. Jacks, "Programs Predict Pressures For Two-Phase Flow," Oil and Gas Journal, $\underline{83}$(37), 93-96 (September 16, 1985).

33) Huntoon, G. C., "Completion Practices in Deep Sour Tuscaloosa Wells," Journal of Petroleum Technology, 33(5), 792-798 (May 1981).

34) Kilstrom, K. J., "Whitney Canyon Sour Gas Well Completion Techniques," Journal of Petroleum Technology, 35(1), 40-46 (January 1983).

35) Lasater, J. A., "Bubble Point Pressure Correlation," Petroleum Transactions of the AIME, 213, 379-381 (1958).

36) Lee, Anthony L., Mario H. Gonzales, and Bertram E. Eakin, "The Viscosity of Natural Gases," Journal of Petroleum Technology, 18(8), 997-1000 (August 1986).

37) Lockhart, R. W., and R. C. Martinelli, "Proposed Correlation of Data for Isothermal Two-Phase, Two-Component Flow in Pipes", Chemical Engineering Progress, 45(1), 39-48 (January 1949).

38) Mateer, Mark W., Personal communication, ARCO Oil and Gas Company, Materials Technology Group, Plano, Texas (August 1987).

39) McNally, Rich, and Mary Jane Ellis, "132 Ultradeep Wells Cost $1.5 Billion," Petroleum Engineer International, 55(3), 43-48 (March 1983).

40) Milligan, M. R., "Sour Gas Well Completion Practices in the Foothills, Western Canada," Journal of Petroleum Technology, 34(9), 2113-2124 (September 1982).

41) Mukherjee, H., and J. P. Brill, "Pressure Drop Correlations for Inclined Two-Phase Flow," Journal of Energy Resources Technology, 107(12), 549-554 (December 1985).

42) Orkiszewski, J., "Predicting Two-Phase Pressure Drops in Vertical Pipe," Journal of Petroleum Technology, 19(6), 829-838 (June 1967).

43) Odell, Peter R., "Oil and World Power," 4th Edition, Penguin Books Ltd., Harmondsworth, Middlesex, England (1975).

44) Parker, Jerald D., James H. Boggs, and Edward F. Blick, "Introduction to Fluid Mechanics and Heat Transfer," Addison-Wesley, Reading, Massachusetts (1974).

45) Poettmann, Fred H., and Paul G. Carpenter, "The Multi-phase Flow of Gas, Oil, and Water Through Vertical Flow Strings with Application to the Design of Gas-Lift Installations," API Drilling and Production Practices, 257-317 (1952).

46) Reid, Robert C., and Thomas K. Sherwood, "The Properties of Gases and Liquids: Their Estimation and Correlation," 2nd Edition, McGraw-Hill, New York, New York (1966).

47) Reinhardt, J. R., and T. S. Powell, "Corrosion Reduction in Production Tubing with the Aid of a Phase Equilibrium Model," OTC 5267, Presented at the 18th Annual Offshore Technology Conference, Houston, Texas (May 1986).

48) Reinicke, K. M., R. J. Remer, and G. Hueni, "Comparison of Measured and Predicted Pressure Drops in Tubing for High-Water-Cut Gas Wells," SPE Produciton Engineering, $\underline{2}$(3), 165-177 (August 1987).

49) Robertson, Carl A., "The Conceptual Development of a Computer Program for the Prediction of Condensation Corrosion in Deep Hot Gas Wells," Report for CHENG 4990, Oklahoma State University, Stillwater, Oklahoma (May 5, 1986).

50) Salama, M. M., and E. S. Venkatesh, "Evaluation of API RP-14E Erosional Velocity Limitations for Offshore Gas Wells," OTC 4485, Presented at the Fifteenth Annual Offshore Technology Conference, Houston, Texas (May 1983).

51) Soave, G., "Equilibrium Constants from a Modified Redlich-Kwong Equation of State," Chemical Engineering Science, $\underline{27}$(6), 1197-1203 (June 1972).

52) Standing, M. B., "A Pressure-Volume-Temperature Correlation for Mixtures of California Oil and Gases," API Drilling and Production Practices, 275-286 (1947).

53) Taitel, Yehuda, Dvora Barnea, and A. E. Dukler, "Modelling Flow Pattern Transitions for Steady Upward Gas-Liquid Flow in Vertical Tubes," AIChE Journal, $\underline{26}$(3), 345-354 (May 1980).

54) Teevens, Patrick J., "Corrosion Control Considerations for the Production of Very (Super) Sour Gas Wells (H_2S > 60 mol%)," Paper No. 47, Presented at Corrosion 87, San Francisco, California (March 15-19, 1987).

55) Tek, M. Rasin, "Multiphase Flow of Water, Oil and Natural Gas Through Vertical Flow Strings," Journal of Petroleum Technology, 13(10), 1029-1036 (October 1961).

56) Tuttle, R. N., "Corrosion in Oil and Gas Production," Journal of Petroleum Technology, 39(7), 756-762 (July 1987).

57) Tuttle, R. N., and T. W. Hamby, "Deep Wells - A Corrosion Engineering Challenge," Materials Performance, 16(10), 9-12 (October 1977).

58) Vazquez, Milton, and H. Dale Beggs, "Correlations for Fluid Physical Property Prediction," Journal of Petroleum Technology, 32(6), 968-970 (June 1980).

59) Wallis, G. B., "One Dimensional Two Phase Flow," McGraw-Hill, New York, New York (1969).

60) West E. H., and John H. Erbar, "An Evaluation of Four Methods of Predicting the Thermodynamic Properties of Light Hydrocarbon Systems," in Proceedings of the Fifty-Second Annual Convention, Gas Processors Association, Dallas, Texas (March 14-16, 1972).

61) Yao, S. C., and N. D. Sylvester, "A Mechanistic Model for Two-Phase Annular-Mist Flow in Vertical Pipes," AIChE Journal, 33(6), 1008-1012 (June 1987).

62) Zigrang, D. J., and N. D. Sylvester, "Explicit Approximations to the Solution of Colebrook's Friction Factor Equation," AIChE Journal, 28(3), 514-515 (May 1982).

63) _____, "Corrosion Control in Petroleum Production," National Association of Corrosion Engineers, Houston, Texas, (1977).

VITA 2

Carl A. Robertson

Candidate for the Degree of

Master of Science

Thesis: DOWN*HOLE, PHASE I: A COMPUTER MODEL FOR PREDICTING THE WATER PHASE CORROSION ZONE IN GAS AND CONDENSATE WELLS

Major Field: Chemical Engineering

Biographical:

Personal Data: Born in Ponca City, Oklahoma, January 24, 1964, the son of Dennis and Jean Robertson.

Education: Graduated from Ponca City Senior High School, Ponca City, Oklahoma, in May, 1982; received Bachelor of Science Degree in Chemical Engineering from Oklahoma State University in December, 1986; completed requirements for the Master of Science Degree at Oklahoma State University in July, 1988.

Professional Experience: Currently employed at the ARCO Oil and Gas Company Production Research Center, Plano, TX, in the Materials Technology Group. Previous experience includes Research Assistant, School of Chemical Engineering, Oklahoma State University, Stillwater, Oklahoma, from January, 1987, to April 1988, and from May, 1986, to August, 1986. Summer Engineer, ARCO Oil and Gas Company, Plano, Texas, May, 1987, to August, 1987. Summer Production Engineer, Amoco Production Company, Farmington, New Mexico, May, 1985, to August, 1985. Summer Engineer, Conoco Inc. Ponca City Refinery, Ponca City, Oklahoma, from May, 1984 to August 1984, and from May, 1983, to August, 1983. Draftsman, Heater Technology Inc., Ponca City, Oklahoma, March, 1980, to May, 1983.